THE JOURNAL OF PHYSICAL CHEMISTRY C
A JOURNAL OF THE AMERICAN CHEMICAL SOCIETY

pubs.acs.org/JPCC

Article

Band Gap Modeling of Different Ternary and Quaternary Alumina Garnet Phases $Y_3(Al_xGa_{1-x})_5O_{12}$ (YAGG) and $Lu_3(Al_xGa_{1-x})_5O_{12}$ (LuAGG). A Semiempirical Approach

Francesco Di Quarto,* Andrea Zaffora, Francesco Di Franco, and Monica Santamaria

Cite This: https://doi.org/10.1021/acs.jpcc.2c04523

Read Online

ACCESS | Metrics & More | Article Recommendations | Supporting Information

ABSTRACT: A further generalization to quaternary oxide systems of the modeling equation of optical band gap values, based on the semiempirical correlation between the differences in the electronegativity of oxygen and the average cationic electronegativity, proposed some years ago, has been carried out by expanding the approach recently employed for ternary mixed oxides. The choice of oxide polymorphs and their influence on the fitting procedure of an experimental data set is evidenced by a detailed discussion of the fitting process of the literature's experimental band gap data pertaining two quaternary oxide systems of the garnet family, namely, $Y_3(Al_xGa_{1-x})_5O_{12}$ (YAGG) and $Lu_3(Al_xGa_{1-x})_5O_{12}$ (LuAGG), playing an important role in several engineering applications. The two investigated systems, moreover, span a quite large range of band gap energy values (from ~5.5 to ~7.5 eV), as a function of the Al/Ga ratio, allowing a rigorous test of the proposed modeling equation. Based on the wide existing literature on the presence of excitonic effects in the investigated systems some empirical correlations between an optical gap and a band gap in the presence of excitonic effects are suggested, too, which could provide some rationale to overcome the discrepancies frequently encountered in comparing band gap values reported in the literature for the same materials. The results of this work confirm the ability of this semiempirical approach in providing good agreement between experimental and theoretical band gap values also for very complex systems, where more sophisticated density functional theory-based methods face some difficulties in predicting the correct values.

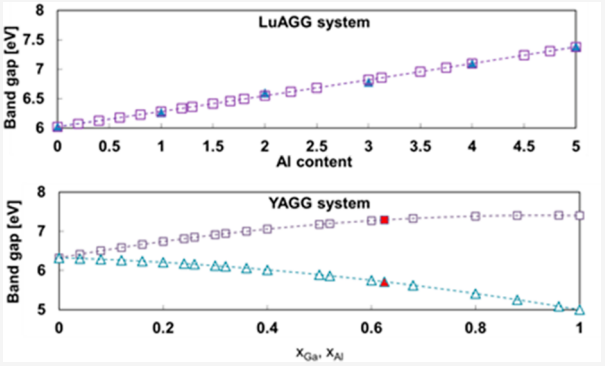

1. INTRODUCTION

The modeling of the optical band gap of semiconducting and insulating materials has been, during the years, one of the main tasks of materials scientists owing to the growing importance of such materials in many fields of the engineering sciences. Although the general task of predicting the band gap of a material is still a formidable task, also for the most advanced quantum mechanical methods rooted in density functional theory, we have shown that it is possible to derive quite realistic values of an optical band gap for relatively complex oxide systems by using a semiempirical approach proposed by the present authors some years ago for binary s,p-metal and d-metal oxides.[1] In that work we showed that it was possible to correlate semiempirically the optical band gap values of numerous crystalline binary oxides to their composition by means of a general expression as

$$E_g = A(\chi_O - \chi_M)^2 + B \quad (1)$$

where χ_M and χ_O are the electronegativities (ENs) of metal and oxygen, respectively, in Pauling's scale. A and B have been determined by a linear best-fitting procedure of experimental E_g values versus $(\chi_O - \chi_M)^2$. In the case of pure s,p- and d-metal oxides two different interpolating straight lines were derived with

$$A_{s,p\text{-met}} = 2.17 \text{ and } B_{s,p\text{-met}} = -2.71 \text{ in eV} \quad (2)$$

for s,p-metal oxides and

$$A_{d\text{-met}} = 1.35 \text{ and } B_{d\text{-met}} = -1.49 \text{ in eV} \quad (3)$$

for d-metal oxides.

eqs 1,2 and eqs 1,3 were used to fit with reasonable accuracy, apart from some discussed exceptions, the optical band gap values, $E_{g,opt}$, of binary sp-metal oxides (II and XIII-XV groups in the periodic table of the elements) and of d-metal oxides (III-XII groups),[2,3] respectively.

Received: June 29, 2022
Revised: September 16, 2022

More recently we extended such a semiempirical approach to pseudoregular (mixed s,p-s,p or d,d-metal oxides) and nonregular (s,p,d-metal oxides) ternary oxides by taking, also, into account the possible changes of band gap values for oxide systems presenting different polymorphs.[4,5] A preliminary test on the reliability of such an approach has been carried out by modeling crystalline pseudoregular ternary systems of different polymorphs α-$(Ga_{(1-x)}Al_x)_2O_3$ and β-$(Ga_{(1-x)}Al_x)_2O_3$ as well as nonregular amorphous ternary systems formed by amorphous mixed oxides, $(Nb_{(1-x)}Al_x)_2O_{(5-2x)}$, $Ta_{(1-x)}Al_x)_2O_{(5-2x)}$, and $W_{(1-x)}Al_{2x}O_3$, obtained by anodizing Al−Nb, Al−Ta, and Al−W metallic alloys at different compositions.[5]

In this work we will extend our semiempirical approach to the modeling of the band gap of multinary oxides by discussing extensively some selected quaternary oxides for which the measured E_g value is of the charge-transfer type; that is, $E_{gap} \propto \Delta$, where the Δ term is directly related to the electronegativity of the anion and the Madelung potential of the solid.[6,7] At this aim, the validity of quaternary oxides band gap modeling equations will be tested against aluminum garnets having general formula $Y_3(Al_xGa_{1-x})_5O_{12}$ (YAGG) and $Lu_3(Al_xGa_{(1-x)})_5O_{12}$ (LuAGG) and covering, according to the literature data,[8−13] a quite large range of band gap values (from ∼5.5 to ∼8.5 eV). The choice of these quaternary oxides was due to

(a) their wide use in technologically relevant applications such as light-emitting diodes (LEDs), plasma display panels, and scintillator materials for medical imaging techniques.

(b) the large amount of experimental data and theoretical models published, through the years, by different research groups allowing a reliable test of the proposed approach with respect to the experimental data as well as in comparison with other approaches based on first principles like the density functional theory (DFT)-rooted theoretical models.[13]

The final aim of this work is to show that the proposed semiempirical approach is capable to provide, in a simple way, useful insights into the band gap of different oxides of relevant interest in several engineering applications.

2. MODELING THE OPTICAL BAND GAP OF MULTINARY OXIDES SYSTEMS

As evidenced from the formula of garnets, $RE_3(Al_xGa_{(1-x)})_5O_{12}$ (with RE = Y, Lu), such a general formula represents a quaternary oxide of variable composition for any value of x ($0 < x < 1$) different from $x = 1$ and $x = 0$, while the end terms of YAGG and LuAGG garnets are coincident with the ternary oxides $Y_3Al_5O_{12}$, $Y_3Ga_5O_{12}$ and $Lu_3Al_5O_{12}$, $Lu_3Ga_5O_{12}$, respectively. According to this the modeling equations for ternary oxides, derived in our recent work[5] and accounting both for the composition and the crystallographic structure of pure and mixed oxides, will be employed to estimate the band gap value of the four end terms of YAGG and LuAGG mixed oxides. As for the quaternary oxides the modeling equations of these more complex systems will be derived in the following by using the same procedure employed for ternary oxide systems.

2.1. Ternary Oxide System. As extensively discussed in our previous works,[4,5] the modeling of the band gap of ternary oxides, $E_{g,T}$, has been carried out by using as starting equations the relationships

$$E_{gT} = x_1E_{g,1}(\chi_{av}) + x_2E_{g,2}(\chi_{av}) = E_{g,2}(\chi_{av}) + x_1(E_{g,1}(\chi_{av}) - E_{g,2}(\chi_{av})) \quad (4)$$

where

$$E_{g,1}(\chi_{av}) = A_1(\chi_O - \chi_{av})^2 + B_1 \quad (5a)$$

and

$$E_{g,2}(\chi_{av}) = A_2(\chi_O - \chi_{av})^2 + B_2 \quad (5b)$$

with

$$\chi_{av} = x_1\chi_1 + x_2\chi_2 \text{ and } x_1 + x_2 = 1 \quad (5c)$$

with x_i and χ_i representing the cationic fraction (in atom %) and Pauling's electronegativity parameter, respectively, of each metal M_i present in the mixed oxides. $E_{g,1}$ and $E_{g,2}$ represent the band gap values of pure binary oxides assumed to follow one of the two previous correlations (sp-sp or d-d-metal) according to eqs 1−3. By substitution of eqs 5a−5c in eq 4 and after simple algebraic manipulations, we got the modeling equation for ternary oxide system as

$$E_{gT,}(\chi_{av}) = E_{g,2} + S_1x_1 + S_qx_1^2 + S_cx_1^3 \quad (6a)$$

where $E_{g,2}$ is the band gap of the pure oxide corresponding to $x_1 = 0$, and

$$S_1 = 2A_2(\chi_O - \chi_2)(\chi_2 - \chi_1) + (B_1 - B_2) + (A_1 - A_2)(\chi_O - \chi_2)^2 \quad (6b)$$

$$S_q = 2(A_1 - A_2)(\chi_O - \chi_2)(\chi_2 - \chi_1) + A_2(\chi_1 - \chi_2)^2 \quad (6c)$$

$$S_c = (A_1 - A_2)(\chi_1 - \chi_2)^2 \quad (6d)$$

eqs 6a−6d represent general relationships used for modeling ternary systems where one or both pure oxides exist as different polymorphs spanning a large range of optical band gap values, which cannot be accommodated in the initial correlation (see eq 1) by keeping constant the A and B parameters reported in eqs 2 & 3 and by varying the Pauling's electronegativity parameter within the accepted uncertainty ($\chi = \chi^0 \pm 0.05$).[5,14] According to this, in the fitting procedure, band gap values derived for different polymorphs of yttria (c-Y_2O_3, m-Y_2O_3, hex-Y_2O_3) and lutetia (c-Lu_2O_3, m-Lu_2O_3, hex-Lu_2O_3) (see below) will be used together with the E_g values previously reported for different alumina and gallia polymorphs.[5] Further detailed information on the fitting procedure of regular and nonregular ternary oxide systems can be found in our previous work.[5]

2.2. Modeling of Nonregular Quaternary Oxides (sp,d-metal mixed oxides). As for the band gap modeling of quaternary oxides, we need to extend our semiempirical approach, previously employed in modeling the optical band gap of ternary oxides, to the case of quaternary oxides. In this paper we will limit ourselves to the quaternary oxide systems of general formula $RE^N(M^1_xM^2_{(1-x)})_5O_{12}$, with RE = (Y, Lu), M^1 = Al, and M^2 = Ga, but the fitting equations can be easily modified to account for different stoichiometry of other nonregular or regular quaternary oxides systems.

By following the strategy used for nonregular ternary oxide systems we assume as starting equation for quaternary oxide systems

https://doi.org/10.1021/acs.jpcc.2c04523
J. Phys. Chem. C XXXX, XXX, XXX−XXX

$$E_{g,q} = \{A_{q,av}(\chi_O - \chi_{q,av})^2 + B_{q,av}\} \quad (7)$$

where χ_O is the electronegativity of oxygen and $A_{q,av}$, $\chi_{q,av}$, and $B_{q,av}$ represent the averaged parameters calculated as below reported

$$A_{q,av} = \frac{A_2^{M_2} \times m(1 - x_1)}{m + n} + \frac{A_1^{M_1} \times mx_1}{m + n} + \frac{A^N \times n}{m + n} \quad (7a)$$

with $(x_1 + x_2) = 1$, $m_2 = m(1 - x_1)$; $m_1 = mx_1$; $n = 3$; $m = 5$.

$$\text{for } x_1 \to 0 \quad A_{q,av} = A_{q,av2} = A_{av,T2} = \frac{A_2^{M_2} m}{m + n} + \frac{A^N \times n}{m + n}$$

$$\text{for } x_1 \to 1 \quad A_{q,av} = A_{q,av1} = A_{av,T1} = \frac{A_1^{M_1} m}{m + n} + \frac{A^N \times n}{m + n}$$

$$B_{q,av} = \frac{B_2^{M_2} \times m(1 - x_1)}{m + n} + \frac{B_1^{M_1} \times mx_1}{m + n} + \frac{A^N \times n}{m + n} \quad (7b)$$

with $(x_1 + x_2) = 1$, $m_2 = m(1 - x_1)$; $m_1 = mx_1$; $n = 3$; $m = 5$.

$$\text{for } x_1 \to 0 \quad B_{q,av} = B_{q,av.2} = B_{av,T2} = \frac{B_2^{M_2} m}{m + n} + \frac{A^N \times n}{m + n}$$

$$\text{for } x_1 \to 1 \quad B_{q,av} = B_{q,av.1} = B_{av,T1} = \frac{B_1^{M_1} m}{m + n} + \frac{A^N \times n}{m + n}$$

$$\chi_{q,av} = (n\chi^N + mx_1 \times \chi^{M1} + m(1 - x_1) \times \chi^{M2})/(m + n)$$
$$= \chi_{2av}(T_2) + x_1 \times (\chi_{1av}(T_1) - \chi_{2av}(T_2)) \quad (7c)$$

where $\chi_{2av}(T_2) = (n \times \chi^N + m\chi^{M2})/(m + n)$ and $\chi_{1av}(T_1) = (n \times \chi^N + m\chi^{M1})/(m + n)$.

After unduly long, but simple, algebraic manipulation we can rewrite eq 7 as

$$E_{g,q}(\chi_{av}) = E_{g,T2} + S_l(q)x_1 + S_q(q)x_1^2 + S_c(q)x_1^3$$
$$\text{with } 0 \le x_1 \le 1 \quad (8)$$

where

$$E_{g,T2} = A_{2,av}(T_2)(\chi_O - \chi_{2,av})^2 + B_{2,av}(T_2) \quad (8a)$$

is the band gap of the ternary systems $(Y,Lu)_3Ga_5O_{12}$ (i.e., YGG and LuGG, respectively) corresponding to $x_1 = 0$. The coefficients of the cubic eq (eq 8) are now written as

$$S_l(q) = 2A_{2T,av}(\chi_O - \chi_{T2,av})(\chi_{T2,av} - \chi_{T1,av}) + (B_{1T,av} - B_{2T,av}) + (A_{1T,av} - A_{2T,av})(\chi_O - \chi_{T2,av})^2 \quad (8b)$$

$$S_q(q) = 2(A_{1T,av} - A_{2T,av})(\chi_O - \chi_{T2,av})(\chi_{T2,av} - \chi_{T1,av}) + A_{2T,av}(\chi_{T1,av} - \chi_{T2,av})^2 \quad (8c)$$

$$S_c(q) = (A_{1T,av} - A_{2T,av})(\chi_{T1,av} - \chi_{T2,av})^2 \quad (8d)$$

The parameters $(A_{1T,av}/A_{2T,av})$ and $(B_{1T,av}/B_{2T,av})$ to be used in eqs 8b–8d are the weighted atom % average of A_i, B_i, and χ_i parameters of ternary end terms of the YAGG and LuAGG garnets (see eqs 7a and 7c), corrected for the different polymorphs[5] (see also below), of the two ternary subsystems pertaining to $x_1 = 0$ and $x_1 = 1$. According to this we will carry out a correction to the B_q parameter value derived from eqs 2 & 3, whenever reliable data on unit volumes are at our disposal and in the presence of appreciable variation in the volume ratio of the different polymorphs of each ternary subsystem. We will come back to these aspects in modeling the band gap of quaternary systems as a function of the oxide composition. We like to stress that, by direct comparison, term to term, of quaternary (eq 8) and ternary (eqs 6a–6d) modeling equations, it comes out that the only difference in the two fitting equations pertains to the substitution of averaged ternary quantities in eq 8, for the definition of the new A, B, and χ parameters of eq 1, with respect to the use in eq 6 of the analogous quantities valid for binary oxide.

3. BAND GAP ESTIMATION OF Y_2O_3 AND LU_2O_3 POLYMORPHS AND TERNARY (Y,LU)-ALUMINATES AND GALLATES (YAG, YGG, LUAG, LUGG)

In recent works[4,5] we discussed the limitations embodied in eq 1 to account for the large differences in band gap values reported in the literature for different oxide polymorphs and how to extend the use of eq 1 in the presence of different polymorphs. In ref 5 we described how to overcome such limitations by discussing, extensively, the case of alumina polymorphs spanning a quite large range of band gap values, from about 4.5 eV for η-Al_2O_3 up to about 8.5–9.0 eV for a-Al_2O_3, as well as the case of gallia ($\alpha,\beta,\gamma,\kappa$-$Ga_2O_3$) polymorphs spanning a much shorter range of $E_{g,opt}$ values. In such work we evidenced the dependence of the B term in eq 1 from the formula unit volume and how to derive a more appropriate value of the B term for all different polymorphs of each oxide. According to our semiempirical approach, the corresponding changes in the value of the A term of eq 1 were determined, for alumina and gallia polymorphs, by using the experimental (or theoretically in a few cases) band gap values reported in the literature. We like to stress that, in using eq 1, a constant value of Pauling's electronegativity of the metallic cation was assumed for all polymorphs. In the following we present results pertaining to yttria and lutetia polymorphs to be employed in the band gap determination and fitting process of (Y,Lu)-aluminates and YAGG and LuAGG garnets.

3.1. Band Gap Estimation of Y_2O_3 and Lu_2O_3 Polymorphs. To calculate the band gap of ternary garnets (YAG, YGG, LuAG, LuGG), according to eqs 6a–6d, we need to derive the band gap values of different binary Y_2O_3 and Lu_2O_3 oxide polymorphs entering in the ternary system. In Tables 1 & 2 of ref 5 we reported the A and B values for different alumina and gallia polymorphs; in this section we will derive the band gap of different yttria (Y_2O_3) and lutetia (Lu_2O_3) polymorphs by following the same approach followed in ref 5.

In agreement with the procedure described in previous works[4,5] we will use the Pauling scale[14−16] of EN by assuming for Y and Lu metals the values $\chi_Y = 1.2 \pm 0.05$ and $\chi_{Lu} = 1.17 \pm 0.05$ by accepting a difference of 0.03 units, in the EN value of Y and Lu metal, equal to that (0.03) reported in the Allen scale[17] of EN but within the accepted uncertainty of Pauling's scale. We must say that, in other EN scales, a larger electronegativity value has been assigned to Lu with respect to Y and, more recently, also in the Rahm-Hoffman EN scale[18] based on Allen's ideas too. We are aware that the intrinsic

https://doi.org/10.1021/acs.jpcc.2c04523
J. Phys. Chem. C XXXX, XXX, XXX−XXX

uncertainty in EN values of the elements, on the order of ±0.05 units usually associated with the Pauling scale of EN, makes our assignment questionable too. However, in agreement with the experimentally higher values of band gap reported in the literature for $Lu_3Al_5O_{12}$ (LuAG) and $LuAlO_3$ (LuAP) with respect to the isostructural ternary oxides $Y_3Al_5O_{12}$ (YAG) and $YAlO_3$ (YAP),[8−13] we will assign the lower value of electronegativity to Lu with respect to Y. Further support for our choice will be provided in deriving the optical band gap of yttria and lutetia (see below).

According to the literature both oxides display a quite similar thermodynamic, electronic, and optical behavior usually discussed within the group of rare-earth sesquioxides for which three different polymorphs have been identified as stable phases in different ranges of temperatures and pressures.[19−26] In the case of yttria and lutetia the stable phase, under ordinary conditions of pressure and temperature, are the cubic and monoclinic phase for which different band gap values have been reported in the literature (see Tables S1 and S2). As for the hexagonal phase no experimental band gap values have been reported in the literature for both oxides, as far as we know, although a value of 5.80 eV for h-Lu_2O_3 is reported in ref 40.

To estimate the optical band gap of yttrium and lutetium oxides the usual A value of transition-metal oxides (A = 1.35, see eq 3) will be assumed for all polymorphs, while the value of B = −1.50 eV, typical of transition-metal oxides, will be assigned only to the more compact hexagonal phases for which reliable volumes for a unit formula, under ordinary conditions of temperature and pressure, have been reported in literature.[25]

The value of B, for cubic and monoclinic polymorphs, will be derived in agreement with the approach reported in ref 5, by using the following equation

$$B^{h} = B^{c,m} + (R_{(c-MOy)}/y) \times [1 - (V_{f.u.}^{c,m}/V_{f.u.}^{h})^{2/3}] \quad (9)$$

where B^h, B^m, B^c and $V_{f.u.}^{h}$, $V_{f.u.}^{m}$, $V_{f.u.}^{c}$ represent the B parameter and the unit formula volume, $V_{f.u.}$, of hexagonal, monoclinic, and cubic yttria (or lutetia) phases, respectively. As reported in Table S1, different B values can be derived, according to the previous equation, for different polymorphs. The highest B value is then derived for the most compact polymorph, that is, hexagonal phase for Y_2O_3 and Lu_2O_3. The experimental unit formula volumes, $V_{f.u}^{i}$, have been used or values derived by reliable DFT-based studies reported in the literature.[20−22] In agreement with the data reported in refs 24 and 25 for yttria polymorphs, the unit formula volume values of $V_{f.u.}^{h\text{-}Y2O3}$ = 66.78 Å^3, $V_{f.u.}^{m\text{-}Y2O3}$ = 68.55 Å^3, and $V_{f.u.}^{c\text{-}Y2O3}$ = 74.56 Å^3, obtained as average of experimental data in cited references, were used in eq 9 for yttria polymorphs. The repulsive energy term,[5] $R = (U_M - U_L)$, was calculated by using for Y_2O_3 the values of Lattice and Madelung energy equal to 12.705 kJ/mol[26,37] (U_L) and 15.206 kJ/mol[38] (U_M), respectively. From eq 9 a value of B = −0.84 eV was derived for c-Y_2O_3 by assuming for the repulsive energy term, $R_{(c\text{-}MOy)}/y$, the value of 8.64 eV. As for the monoclinic phase a value of B = −1.34 eV was derived, from eq 9, for the m-Y_2O_3 polymorph. By using A = 1.35 and χ_Y = 1.2, for yttria phases, band gap values of 5.64, 5.80, and 6.30 eV are derived for h-Y_2O_3, m-Y_2O_3, and c-Y_2O_3, respectively. The highest band gap value is in very good agreement with the room-temperature band gap values reported in the literature for single-crystal c-Y_2O_3.[9,27,28] The value of 5.80 eV is also in good agreement with the $E_{g,opt}$ values (5.68−5.88 eV) reported for monoclinic powders.[29] Both values are, also, in good agreement with band gap values of yttria theoretically derived by using a DFT-based method.[30−34] As for h-Y_2O_3 we are not aware of any experimental E_g value reported in the literature for this polymorph, while E_g values around 5.62 eV have been estimated by DFT-methods also for c-Y_2O_3.[35] Although it is confirmed the usual scattering of experimental band gap values as a function of sample preparations and techniques of investigation, the literature data seem to confirm an appreciably higher band gap value for c-Y_2O_3 with respect to the monoclinic polymorph as suggested in our semiempirical approach. Further experimental band gap data on h,m-Y_2O_3 polymorphs could help to assess the limits of validity of our suggested approach. In Table S1 we summarized all the data pertaining to the formula unit volumes and B parameter as well as estimated and experimental band gap values.

By following the same procedure for Lu_2O_3, values of B = −1.14, −1.44, and −1.50 eV have been derived, according to eq 9, for different polymorphs by using unit formula volumes equal to 70.03, 65.37, and 64.47 Å^3 for c-Lu_2O_3, m-Lu_2O_3, and h-Lu_2O_3, respectively. As for the cubic polymorph the reported value of formula unit volume is the average of experimental values reported in refs 22 and 36 while in the case of the other two polymorphs they are DFT calculated values as reported in refs 21 and 41.

A repulsive energy term, $R_{(c\text{-}MOy)}/y$, equal to 6.40 eV was used in eq 9 in agreement with the reported values of 13.665 kJ/M for the lattice energy[37] (U_{Latt} = 13.665 kJ/M) and of 15.520 kJ/M for the Madelung energy (U_M = 15.520 kJ/M).[38] By assuming for Lu an EN value χ_{Lu} = 1.17, band gap values of 5.83, 5.89, and 6.19 eV have been derived for hexagonal, monoclinic, and cubic phases, respectively, of Lu_2O_3. The lowest value agrees quite well with the optical band gap value (5.50−5.80 eV) reported for h-Lu_2O_3.[39,40] Lower band gap values have been derived by DFT methods for h-Lu_2O_3 polymorph,[41−43] while higher E_g values have been estimated for c-Lu_2O_3.[31,35] As for the experimental data, band gap values ranging from 5.5 to 6.5 eV have been reported in the literature for Lu_2O_3 samples depending both on the nature of samples as well as from the experimental techniques employed.[44−51] As for c-Lu_2O_3 crystalline samples, direct optical band gap values around 5.80−6.0 eV have been frequently reported,[44,45] in good agreement with experimental data derived from electron energy loss spectroscopy (EELS) technique[46−48] and luminescence excitation spectra[49−51] and in quite good agreement with the value above-reported for such a polymorph. The highest band gap values reported[8,52] for c-Lu_2O_3 as well c-Y_2O_3 single crystals have been derived from luminescence excitation spectra once the presence of excitonic effects, near the optical absorption threshold of RE-sesquioxides, is also taken into account.[23,52−54] Unfortunately very few experimental data have been reported for monoclinic and hexagonal lutetia so that the $E_{g,opt}$ data reported in Table S2 for these polymorphs should be taken with some caution.

We like to stress that, as expected according to eq 1, higher band gap values have been obtained for lutetia polymorphs with respect to the corresponding yttria polymorphs; however, the difference of the estimated band gap on going from hexagonal to cubic polymorph decreases until it disappears. It comes out that, in the presence of small differences in the EN values of different cations, further variables depending on the details of crystalline structure of each polymorph can affect the

https://doi.org/10.1021/acs.jpcc.2c04523
J. Phys. Chem. C XXXX, XXX, XXX−XXX

expected trend in band gap values. We will come back to these aspects in the next section in discussing the fitting procedure of ternary oxide systems.

3.2. Band Gap Estimation of Ternary Oxides (YAG, YGG, LuAG, LuGG). The complications arising in comparing, for any assigned material, the E_g data obtained from theoretical models with those experimentally derived, by using different experimental techniques, have been discussed in previous works[4,5] (and refs therein). In the case of large band gap materials, like those investigated in this work, further complications arise from difficulties in deriving reliable room temperature optical band gap values in the presence of interfering excitonic effects.[8−10,13] In these cases we have to distinguish between "the energy of the onset of fundamental absorption E^{fa}",[55,56] practically coincident with the optical band gap (or exciton band gap) $E_{g,opt}$ of the material derived according to one of the usual optical methods,[4,5] and the fundamental electronic band gap. The fundamental band gap of the material can be obtained by summing to the exciton band gap, the electron−hole binding energy of exciton. This last term can be calculated once the static (or low-frequency) dielectric constant and the exciton-reduced effective mass are known.[57,58] Unfortunately, both these parameters, and particularly the exciton-reduced effective mass, are not generally known. According to this, Dorenbos suggested, in the presence of excitonic effects, to correlate the electronic band gap of materials to the peak of exciton energy, if available, through the relationship[10,55,56]

$$E_g(A_aB_bO_o) = E^{exc} + 0.008 \times (E^{exc})^2 \quad (10a)$$

where E^{exc} is the exciton peak energy of the host material, experimentally measured at a given temperature, while the second term represents an estimate of the electron−hole binding energy of excitons. These effects are better evidenced and quantified at very low temperatures (usually around 10 K) and by using high-energy incident photons, usually synchrotron light. In absence of a detailed study on the dependence of E^{exc} from the temperature, a correction of about −0.15 eV, to the E^{exc} value measured at 10 K, has been suggested by Dorenbos[8,55,56] to get the E^{exc} value of YAGG and LuAGG garnets at room temperature (RT). According to this, we will assume

$$E_g = (E^{exc}(10\ K) - 0.15) + 0.008 \times (E^{exc}(10\ K) - 0.15)^2 \text{ at room temperature} \quad (10b)$$

As for the ternary oxides $Y_3Al_5O_{12}$ (YAG) and $Y_3Ga_5O_{12}$ (YGG), experimental optical band gap values around 6.50 and 5.50 eV, respectively, have been reported at room temperature by different authors.[53,59−62] In refs 53 and 59−61 the optical band gap of YAG and YGG was defined as the photon energy corresponding to a light absorption coefficient value of $\alpha = 10\ cm^{-1}$.

As for YGG a value of $E^{exc} = 5.93$ eV, at 8 K, has been reported[63] from which value a band gap of 6.21 eV is obtained, according to eq 10a, in quite good agreement with band gap value reported in the literature for YGG.[11] According to this, by assuming, for YGG, $E^{fa} = E_{g,opt} = 5.50 \pm 0.05$ eV, it is possible to write

$$E^{exc}(10\ K) = (E^{fa}(298\ K) + 0.40eV \quad (10c)$$

which can be rearranged as

$$E^{exc}(298\ K) = E^{exc}(10\ K) - 0.15\ eV = E^{fa}(298\ K) + (0.4 - 0.15)\ eV = E^{fa}(RT) + 0.25(\pm 0.05)\ eV \quad (10d)$$

From eq 10d a difference between E^{exc} (298 K) and E^{fa} (298 K) of 0.25 eV is estimated from the experimental data pertaining to YGG. We have to say that a similar difference of energy value (0.25−0.30 eV) between the host excitation energy peak, E^{exc}, and the fundamental absorption energy onset of the host exciton, E^{fa}, has been experimentally observed for YAG[64] and LuAG,[65] too, at low temperatures (T = 7−10 K) as well as at room temperature (T = 300 K) for antisite defects of the Y_{Al}^{3+} type.[64]

As for YAG, E^{exc} values ranging from 7.10[66] to 6.90 eV[67] have been reported, at 10 K, for pure as well for Ce^{3+} and Pr^{3+} doped YAG single crystals, so that, by assuming an average E^{exc} value of 7.0 ± 0.1 eV, values of $E^{exc}(RT) = 6.85 \pm 0.1$ eV and $E^{fa}(RT) = 6.60 \pm 0.1$ eV are expected, at room temperature for YAG. The $E^{exc}(RT)$ average value is in good agreement with the room temperature value of 6.90 eV reported by Kirm et al.[68] while the $E^{fa}(RT)$ value agrees with the E_{gopt} values, 6.5 eV, of refs.[59,60] From $E^{exc}(RT)$ a band gap value of 7.23 eV ± 0.12 eV, at room temperature, is now derived for YAG by using eq 10a.

The ability of eqs 9 and 10a−10d in providing reasonable values of optical band gap values also for c-Y_2O_3 and c-Lu_2O_3 has been tested by deriving the $E_{g,opt}$ values of both oxides, at room temperature, on starting from the band gap values of 6.30 and 6.20 eV above-reported for the two cubic phases. From eq 10a a value of $E^{exc}(298\ K) = 6.01$ eV is obtained for c-Y_2O_3 from which value an optical band gap $E_{g,opt} = E^{fa} = E^{exc} - 0.25 = 5.76$ eV is derived. The E^{exc} value is in good agreement with the value of the exciton energy peak reported by different authors,[23,53,54,69] while the derived E^{fa} value is in very good agreement with the values of direct optical band gap reported in the literature for cubic-Y_2O_3 ($E_{g.opt}$ = 5.73−5.825 eV).[29,70] Analogously for c-Lu_2O_3 a value of $E^{exc}(RT) = 5.92$ eV is derived from eq 10a from which value an $E_{g.opt}$ value of 5.67 eV is obtained at room temperature. The value of $E^{exc}(RT)$ is in good agreement, too, with the value of exciton energy peak experimentally measured,[23] at 300 K, for a single crystal of c-Lu_2O_3, while the $E_{g.opt}$ value is in good agreement with the values of $E_{g,opt}$ = 5.50−5.80 eV reported in Table S2 for crystalline c-Lu_2O_3 films.[39,44,71g,h]

Although further investigations are mandatory before generalizing the use of eqs 9 and 10a−10d also to lower band gap oxides, in the following, unless differently stated, we will assume $E^{fa} = E_{g,opt}$ while eqs 9 and 10a−10d will be employed to derive the electronic band gap values of the investigated oxides, on starting from the experimental E^{exc} and/or $E_{g,opt}$ values reported in the literature for ternary aluminates and gallates as well for the investigated garnets of general formula $Y_3(Al_xGa_{(1-x)})_5O_{12}$ (YAGG) and $Lu_3(Al_xGa_{(1-x)})_5O_{12}$ (LuAGG).

As for the fitting procedure of ternary and quaternary oxides we must take into consideration that

(a) in our semiempirical approach[1] the A and B parameters of eqs 1 & 2 have been experimentally derived,[1−5] for both d-metal and s,p-metal oxides, by using the optical band gap value of oxides without taking into consideration possible excitonic effects. For oxide polymorphs showing appreciable difference (>0.1 eV)

https://doi.org/10.1021/acs.jpcc.2c04523
J. Phys. Chem. C XXXX, XXX, XXX−XXX

between optical (exciton) and electronic band gap a corresponding change in the A parameter, at fixed B, will be carried out to account for such a difference.

(b) the optical band gap values employed in deriving the initial correlations (see eqs 1 & 2 and ref 1) were usually measured at room temperature and often derived by means of Tauc's plot. This means that, in the presence of excitonic effects, the optical band gap values derived by this technique, assumed as E^{fa} values, could not coincide with a fundamental electronic gap.

In the following, we will assume eqs 10a−10d as good approximations for the estimation of the different characteristic energies, E_g, E^{exc}, and E^{fa}, of ternary and quaternary oxide systems, at room temperature and in the presence of excitonic effects. Further support for the use of such relationships will be provided in the fitting process of experimental data pertaining to the investigated systems.

3.3. Fitting of Band Gap Values of Ternary Oxides (YAG, YGG, LuAG, LuGG). As a preliminary introduction to the fitting procedure of crystalline quaternary systems, we will carry out the fitting of nonregular mixed d-s,p-metal ternary oxides, $(Y,Lu)_3Al_5O_{12}$ and $(Y,Lu)_3Ga_5O_{12}$, corresponding to the end terms of the YAGG and LuAGG garnets. This is a necessary step to derive the band gap values ($E_{g2,T}$ & $E_{g1,T}$) and fitting parameters (A_{2q}, A_{1q} and $B_{2q.av}$, $B_{1q.av}$ see eqs 7a & 7b) to be employed in eqs 8a−8d to fit the band gap behavior of quaternary systems $Y_3(Al_xGa_{1-x})_5O_{12}$ and $Lu_3(Al_xGa_{1-x})_5O_{12}$, where $Y_3Ga_5O_{12}$ and $Lu_3Ga_5O_{12}$ represent the starting points (at $x_{Al} = 0$, $E_{g2,T}$ in eqs 7 & 8) while $Y_3Al_5O_{12}$ and $Lu_3Al_5O_{12}$ ($x_{Al} = 1$, $E_{g1,T}$ in eqs 7,8) represent the end points of the quaternary fitting curves (see below).

In order to test the ability of our approach (see eqs 6a−6d) to estimate the band gap values of the ternary oxides, representing the two end terms of quaternary YAGG, we report in Figure 1 the behavior of $E_{gT}(\chi_{av})$ modeling equation as a function of Al or Ga content in mixed ternary oxides: $(Y_{(1-x)}Al_x)_2O_3$ (squares in Figure 1) and $(Y_{(1-x)}Ga_x)_2O_3$ (triangles in Figure 1). For $x_{Al,Ga} = 0.625$, corresponding to the ratio of Al/(Y + Al) or Ga/(Ga + Y) existing in YAG and YGG, E_{gT} values of 7.28 eV (red square) and 5.70 eV (red triangle) (E^{exc} = 5.46 eV) for YAG and YGG garnets, respectively, are obtained.

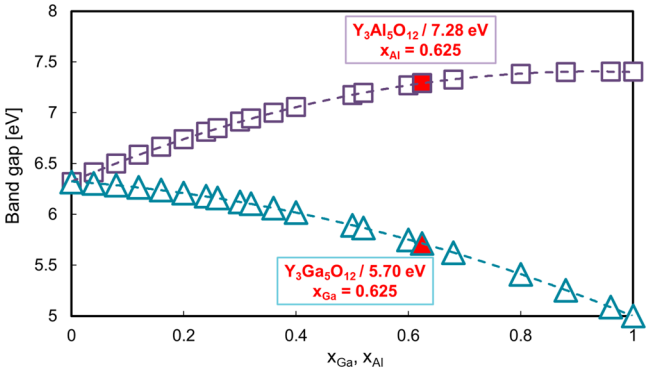

Figure 1. Modeling of the band gap of ternary oxides $(Y_xAl_{(1-x)})_2O_3$ and $(Y_xGa_{(1-x)})_2O_3$ to estimate the E_g values of YAGG end terms $Y_3Al_5O_{12}$ and $Y_3Ga_5O_{12}$ by assuming as binary oxides c-Y_2O_3 and k-Al_2O_3 for the formation of cubic yttrium aluminate (YAG) and c-Y_2O_3 and k-Ga_2O_3 for cubic yttrium gallate (YGG). Theoretical band gap values (square: $0 \le x_{Al} \le 1$) and (triangle: $0 \le x_{Ga} \le 1$) derived according to eqs 6a−6d by assuming for k-Al_2O_3 (see text): χ_{Al} = 1.50; $B_{k\text{-}Al_2O_3}$ = −2.415 eV; $A_{k\text{-}Al_2O_3}$ = 2.455; χ_{Ga} = 1.60; $B_{k\text{-}Ga_2O_3}$ = −2.45 eV; $A_{k\text{-}Ga_2O_3}$ = 2.064; χ_Y = 1.20; $B_{c\text{-}Y_2O_3}$ = −0.84 eV; $A_{c\text{-}Y_2O_3}$ = 1.35.

The E_g value estimated for YAG (7.28 eV) is in very good agreement with the average experimental value (7.23 eV) derived in a previous section. As reported in the caption, the data of $(Y_{(1-x)}Al_x)_2O_3$ (square) have been obtained by using in eqs 6 as E_{g2} value ($x_{Al} = 0$ or $x_{Ga} = 0$) the band gap value of 6.30 eV derived for c-Y_2O_3, together with the corresponding A_2 = 1.35 and B_2 = −0.84 eV parameters. As for E_{g1} the value of 7.40 eV has been used for k-Al_2O_3, together with the corresponding A_1 (2.455) and B_1 (−2.415 eV) parameters, reported in a previous work.[5]

The initial choice of cubic yttria is supported by the fact that, under ordinary conditions of temperature and pressure, c-Y_2O_3 is the stable phase.[20] We have to say that different coordination number to O^{-2} (C.N. = 8) is experienced by Y^{3+} ions in a crystalline YAG structure (dodecahedrically coordinated to O^{-2}) with respect to c-Y_2O_3 where Y^{3+} ions occupy octahedral sites (C.N. = 6).[72,73] As for the aluminum oxide polymorph employed in the fitting process of YAG, we have chosen k-Al_2O_3 polymorph for which theoretical band gap values in the range of 7.40−7.67 eV have been reported in the literature.[74,75] In the YAG structure Al^{3+} ions occupy both tetrahedral (T) as well octahedral (Oct) sites with a fixed ratio of Al^{3+}(Oct)/Al^{3+}(T) = 2/3 (40/60%).[72,73] In k-alumina (75−50%) of Al^{3+} ions occupy octahedral and pentahedral (0−25%) sites, and only 25% occupy tetrahedral sites.[75,76] With the exclusion of α-alumina, where all Al^{3+} ions occupy octahedral sites, all other polymorphs have a variable percentage (>20%) of Al^{3+} ions occupying tetrahedral sites but all display lower band gap values both with respect to k-alumina[5,76,77] and YAG phase.

As for the band gap of YGG (see Figure 1) we followed the same procedure by using, initially, in eq 6a as E_{g1} the optical band gap value of $E_{g,opt}$ = 5.0 eV, in agreement with the experimental range of values (4.95 ± 0.05 eV) reported in the literature for k-Ga_2O_3.[75,78−80] The band gap value of 5.70 eV derived for YGG is appreciably lower than the expected one E_g(RT) = 6.05 eV (see above), while it is higher than the $E_{g,opt}$ value (~5.50 eV) reported in the literature for YGG.[60,62] In order to understand the origin of such discrepancy in the value of E_g for YGG, we decided to estimate the $E_{g,opt}$ value of YGG by using in eqs 6a−6d as E_{g2} the optical band gap of c-Y_2O_3 equal to 5.76 eV, previously determined, together with the new A value (A = 1.248), derived by means of eq 1, and with the value of B = −0.84 eV previously estimated. By leaving unaltered the $E_{g,opt}$ value of k-Ga_2O_3 (5.0 eV), a value of $E_{g,opt}$ = 5.54 eV is now obtained for YGG (see Figure 2) in very good agreement both with the value of $E_{g,opt}$ (5.50 eV) reported in the literature[60,62] as well as with the E^{fa} value (5.53 eV) derived from the E^{exc} value[63] by means of eq 10c.

By using eqs 10a & 10d and the estimated $E_{g,opt}$ = 5.54 eV a value of band gap of 6.06 eV is now derived for YGG. This E_g value is in good agreement with that one previously estimated (6.05 eV) as well with analogous values reported in the literature once the correction for the difference of temperature is carried out.

We, further, tested the hypothesis that the optical band gap value ($E_{g,opt}$ = 4.95 ± 0.05 eV) reported[5] for k-Ga_2O_3 is not the fundamental band gap but an excitonic gap. By assuming $E_{g,opt}$ as a measure of the excitonic gap, that is, E^{fa}, a "fundamental"

https://doi.org/10.1021/acs.jpcc.2c04523
J. Phys. Chem. C XXXX, XXX, XXX−XXX

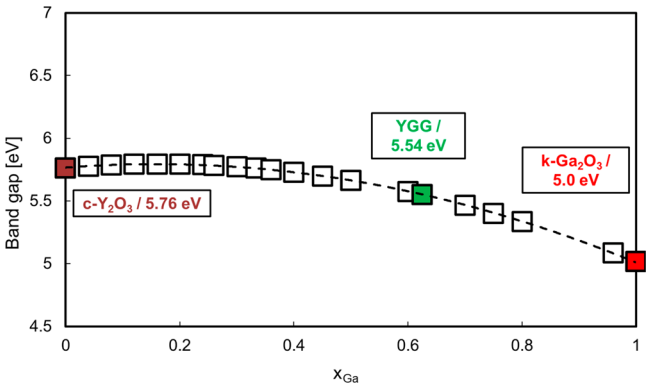

Figure 2. Modeling of the optical band gap of ternary oxides $(Y_xGa_{(1-x)})_2O_3$ to estimate the $E_{g,opt}$ values of YGG ($Y_3Ga_5O_{12}$) by assuming as binary oxides c-Y_2O_3 and k-Ga_2O_3 for cubic yttrium gallate (YGG). Theoretical optical band gap values (square: $0 \le x_{Ga} \le 1$) derived according to eqs 6a−6d and by assuming (see text and Table S1) for c-Y_2O_3: $E_{g,opt}$ = 5.76 eV; χ_Y = 1.20; $B_{c\text{-}Y_2O_3}$ = −0.84 eV; $A_{c\text{-}Y_2O_3}$ = 1.248; and for k-Ga_2O_3: $E_{g,opt}$ = 5.0 eV; χ_{Ga} = 1.60; $B_{k\text{-}Ga_2O_3}$ = −2.45 eV; $A_{k\text{-}Ga_2O_3}$ = 2.064.

electronic band gap of k-Ga_2O_3 can be estimated by means of eqs 10a & 10d as

$$E_g = (E_{g,opt} + 0.25)^2 \times 0.008 + (E_{g,opt} + 0.25) = 5.202 \times 0.008 + 5.20 = 5.42 \pm 0.05 \text{ [eV]} \quad (11)$$

The difference of 0.47 eV between E_g and the excitonic gap, $E_{g,opt}$, is in fair agreement with the estimated binding energy (0.4−0.5 eV) of the lowest exciton in α,β-Ga_2O_3.[81−84] By using, now, in Figure 3 the value of 5.47 as the "fundamental"

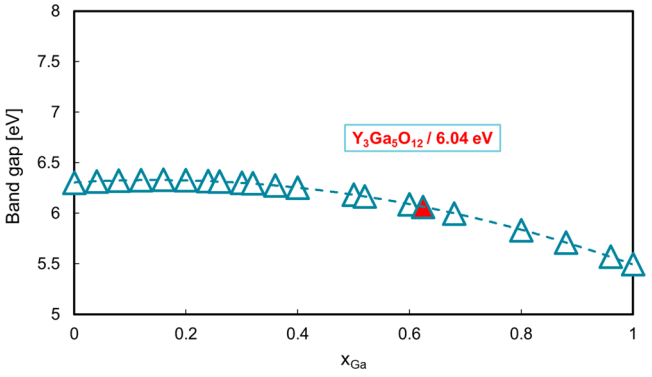

Figure 3. Band gap modeling for ternary oxides $(Y_xGa_{(1-x)})_2O_3$ to estimate the E_g value of YGG ($Y_3Ga_5O_{12}$) by assuming as E_g values for k-Ga_2O_3 the value of 5.47 eV (see text). Theoretical band gap values (triangle: $0 \le x_{Ga} \le 1$) derived according to eqs 6a−6d and by assuming for c-Y_2O_3 E_g = 6.30 eV (see text and Table S1): χ_Y = 1.20; $B_{c\text{-}Y_2O_3}$ = −0.84 eV; $A_{c\text{-}Y_2O_3}$ = 1.35; χ_{Ga} = 1.60; $B_{k\text{-}Ga_2O_3}$ = −2.45 eV; $A_{k\text{-}Ga_2O_3}$ = 2.194.

band gap for k-Ga_2O_3 the theoretical E_{g2T} values (triangles) for ternary $(Y_xGa_{1-x})_2O_3$ mixed oxides have been obtained by keeping as fixed the E_{g2} term in eq 6a the band gap value of c-Y_2O_3 (6.30 eV) and as E_{g1} the fundamental band gap value of 5.47 eV for k-Ga_2O_3.

The room-temperature band gap of YGG, corresponding to x_{Ga} = 0.625, derived from Figure 3 is now 6.04 eV, practically coincident with that previously derived by using eq 10d and the estimated E^{fa} value. As for the A parameter of k-Ga_2O_3 the new value of 2.194 eV, estimated by means of eq 1 and by using the new fundamental band gap value, has been employed in eqs 6a−6d together with the B value of −2.45 eV suggested for k-gallia polymorph in our previous work.[5] The values of parameters employed in the fitting procedure have been reported in the captions of Figures 2 and 3.

By following the same procedure used for YAG and YGG ternary oxides we report in Figure 4 the theoretical E_g values of $(Lu_xAl_{(1-x)})_2O_3$ and $(Lu_xGa_{(1-x)})_2O_3$ as a function of Al and Ga content in the mixed oxides ($x_{Al,Ga} \le 1$).

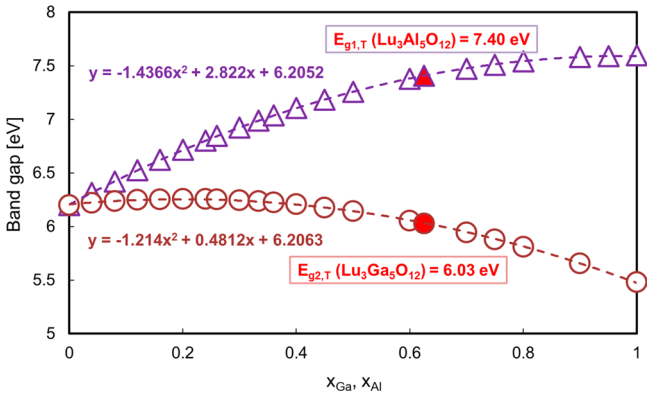

Figure 4. Modeling of band gap of ternary oxides $(Lu_xAl_{(1-x)})_2O_3$ and $(Lu_xGa_{(1-x)})_2O_3$ to estimate the E_g values of LuAGG end terms, $Lu_3Al_5O_{12}$ and $Y_3Ga_5O_{12}$, by assuming as binary oxides c-Lu_2O_3 and k-Al_2O_3 (or k-Ga_2O_3) for the formation of cubic lutetium aluminate (LuAG) or cubic lutetium gallate (LuGG), respectively. Theoretical band gap values (triangle: $0 \le x_{Al} \le 1$) and (circle: $0 \le x_{Ga} \le 1$) derived according to eqs 6a−6d by assuming for k-Al_2O_3 (see text) E_g = 7.60 eV: χ_{Al} = 1.50; $B_{k\text{-}Al2O3}$ = −2.415 eV; $A_{k\text{-}Al_2O_3}$ = 2.50; for k-Ga_2O_3 (see text) E_g = 5.47 eV: χ_{Ga} = 1.60; $B_{k\text{-}Ga_2O_3}$ = −2.45 eV; $A_{k\text{-}Ga_2O_3}$ = 2.194; and for c-Lu_2O_3 = 6.20 eV (see Table S2): χ_{Lu} = 1.17; $B_{c\text{-}Lu_2O_3}$ = −1.14 eV; $A_{c\text{-}Lu_2O_3}$ = 1.35.

The value of 6.03 eV for LuGG ($E_{g2,T}$) and 7.40 eV for LuAG ($E_{g1,T}$) have been obtained, for $x_{Al,Ga}$ = 0.625 and according to eqs 6a−6d, by using for c-Lu_2O_3 the estimated E_{g2} value of 6.20 eV (see Table S2) and for k-Ga_2O_3 and k-Al_2O_3 polymorphs the value of E_{g1} = 5.47 eV and E_{g1} = 7.60 eV, respectively. The E_g values, derived in Figure 4 for LuGG and LuAG, are in good agreement with the band gap values reported in the literature.[11,85] As evidenced in Figure 4 a value of E_{g1} = 7.60 eV for k-Al_2O_3, slightly larger than that one previously employed for modeling the ternary $(Y_xAl_{(1-x)})_2O_3$ system, has been used in modeling the ternary $(Lu_xAl_{(1-x)})_2O_3$ system, while the same value of E_{g1} = 5.47 eV, previously used in Figure 3 for k-Ga_2O_3, has been again employed in modeling the $(Lu_xGa_{1-x})_2O_3$ ternary system. We have to say that the E_g value of k-alumina, although higher than the previous one used in fitting the YAG value, is still lower than the value of 7.67 eV recently estimated for this alumina polymorph.[75]

We like to mention that, by using as the E_g value for k-alumina the E_g values of 7.40 or 7.67 eV estimated by DFT techniques, the range of E_g values derived for LuAG is comprised between 7.28 and 7.46 eV. In both cases the estimated E_g(RT) values, for the LuAGG end term (x = 1), are in good agreement with the experimental band gap values reported in the literature or derived from experimental E^{exc} values by means of eqs10a & 10b (after correction for the

https://doi.org/10.1021/acs.jpcc.2c04523
J. Phys. Chem. C XXXX, XXX, XXX−XXX

difference of temperature where necessary).[65,67,85−88] Analogously the choice of a fundamental band gap value for k-Ga_2O_3 (5.42 ± 0.05 eV) instead of the optical gap ($E_{g,opt}$ = 4.95 ± 0.05 eV) is supported by the good agreement between the estimated E_g values and the band gap values of YGG and LuGG reported in the literature (see also the next section).[8−11]

4. MODELING OF E_G VERSUS X_{AL} DATA FOR $Y_3(GA_{(1-X)}AL_X)_5O_{12}$ (YAGG) AND $LU_3(GA_{(1-X)}AL_X)_5O_{12}$ (LUAGG) GARNET PHASES

To test the validity of our approach in modeling the optical band gap of quaternary oxides by means of eq 8 and eqs 8a−8d) derived in Section 2.2, we selected, for the two investigated quaternary systems, the experimental data set of E^{exc} and/or E_{fa} values covering the largest interval of compositions of both (YAGG, LuAGG) quaternary oxides described in recent literature.[55,56,89]

As for the modeling of YAGG experimental band gap values, we plotted in Figure 5 the room-temperature E^{fa} values of host

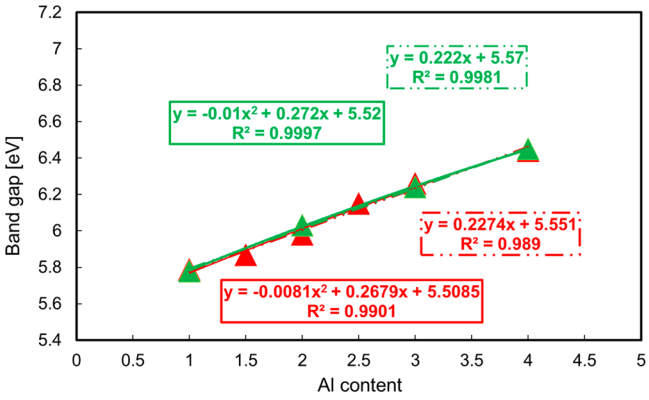

Figure 5. Experimental data sets of E_{fa} values for $Y_3(Al_xGa_{(1-x)})_5O_{12}$) for $1 \le mx_{Al} \le 4$ from refs 55 and 56.

exciton band gaps in YAGG:Ce (red triangles) and YAGG:Pr (green triangles) obtained by using Tauc plots, in the hypothesis of direct allowed transitions, from photoluminescence excitation (PLE) spectra.[55,56]

The E^{fa} values (Figure 5) cover the range of composition going from mx_{Al} = 1 to mx_{Al} = 4, but in the case of YAGG:Ce^{3+}two more values of E^{fa}, at mx_{Al} = 1.5 and mx_{Al} = 2.5, are plotted as reported in the original work.[55] This choice was preferred for two reasons:

(a) for x_{Al} = 0 the E^{fa} value of YGG:Ce^{3+} was not reported in the data set (see table1 of the original work),[55] so that it seemed to us more correct to keep constant the exploited interval of composition of the quaternary system.

(b) for mx_{Al} = 5 the average value of E_{fa} (6.60 ± 0.1 eV), derived by means of eqs 10a−10d by using the range of experimental values reported for E^{exc}, covers also the experimental $E_{g,opt}$ values reported in literature.[56]

As reported in Figure 5, from the linear as well as the quadratic fitting lines on both series of experimental E^{fa} data, a value of E^{fa} = 5.54 eV for YGG (x_{Al} = 0) and of E^{fa} = 6.65 eV for YAG (x_{Al} = 1) is derived, by averaging on both series of data and interpolating fitting lines in good agreement with the $E_{g,opt}$ values reported previously for both end terms of YAGG.[53,56,59−62] We like to stress that the E^{fa} value of YGG derived from the data of Figure 5 is coincident with the $E_{g,opt}$ value derived from Figure 2 by using the modeling equations (see eqs 6a−6d) derived for nonregular ternary systems[5] together with the optical band gap values of c-Y_2O_3 (E_{g2} = 5.76 eV), derived from the estimated E_g value of c-Y_2O_3, and the $E_{g,opt}$ value of k-Ga_2O_3 reported in literature.[75] From these E^{fa} values we can estimate the band gap values of YGG and YAG for the two end terms of YAGG by using eqs 10a & 10d as

$$E_g(\mathrm{YAG}) = (6.65 + 0.25)^2 \times 0.008 + 6.90 = 7.28 \text{ eV for } Y_3Al_5O_{12} \quad (12a)$$

$$E_g(\mathrm{YGG}) = (5.54 + 0.25)^2 \times 0.008 + 5.79 = 6.058 \text{ eV for } Y_3Ga_5O_{12} \quad (12b)$$

We like to stress that the band gap value of the YAGG end term, $Y_3Al_5O_{12}$, derived from eq 12a by using the averaged experimental E^{fa} data of Figure 5, is almost coincident with the E_{g1T} value previously estimated (see Figure 1) by means of eqs 6a−6d and by using the estimated band gap value (6.30 eV) of c-Y_2O_3 (see Table S1) and E_g value (7.40 eV) of k-Al_2O_3 reported in ref 5. On the other hand, the E_g value (6.058 eV) obtained from eq 12b is in good agreement with the value of E_g derived for nonregular ternary systems (see Figure 3) only if we use for k-Ga_2O_3 a "fundamental band gap" value as that derived by means of eq 12b. Although a strong support in favor of the possible presence of an excitonic gap in k-gallia can be traced out to the recent discoveries[81−84] of the existence of excitons in α,β-Ga_2O_3 as well as to the similarity of the band

Table 1. Experimental E^{fa} and E^{exc} and Calculated E_g Values of $Y_3(Ga_{1-x}Al_x)_5O_{12}$ from eqs 8 and 10a (see Figures 5 & 6 and the Text)[a]

x_{Al}	$Y_3(Ga_{1-x}Al_x)_5O_{12}$	E_{exp}^{fa} (298 K)[55]	E_{corr}^{fa} (298 K)	E_{exp}^{fa} (10 K)[56]	E_{exp}^{exc} (10 K)	$E_{exp,av}^{exc}$ (298 K)	$E_{g,calc}$ (298 K) from eq 10a	$E_{g,th}$ (298 K) from eq 8
0	$Y_3Ga_5O_{12}$				5.93[63]	5.78	6.05	6.04
1	$Y_3Ga_4AlO_{12}$	5.79	5.81	5.96		6.05	6.34	6.28
1.5	$Y_3Ga_{3.5}Al_{1.5}O_{12}$	5.87				6.12	6.42	6.40
2	$Y_3Ga_2Al_2O_{12}$	5.98	6.06	6.21		6.27	6.58	6.53
2.5	$Y_3Ga_{2.5}Al_{2.5}O_{12}$	6.15				6.40	6.73	6.65
3	$Y_3Ga_2Al_3O_{12}$	6.26	6.27	6.42		6.515	6.85	6.78
4	$Y_3Ga_1Al_4O_{12}$	6.44	6.48	6.63		6.71	7.07	7.05
5	$Y_3Al_5O_{12}$					6.90	7.28	7.28

[a]All the band gap values are expressed in electronvolts. $E_{exp,av}^{exc}$ = 6.90 eV is the averaged value between those reported in refs 65, 66, 68, and 97−100.

https://doi.org/10.1021/acs.jpcc.2c04523
J. Phys. Chem. C XXXX, XXX, XXX−XXX

gap structures of different Ga_2O_3 polymorphs, we have to say that the assumption of a fundamental band gap in k-gallia still needs further experimental confirmation.

In Table 1 experimental and theoretical band gap values related to YAGG compounds are summarized.

As for the modeling of the YAGG quaternary system, we report in Figure 6 the experimental, at room temperature, E^{fa}

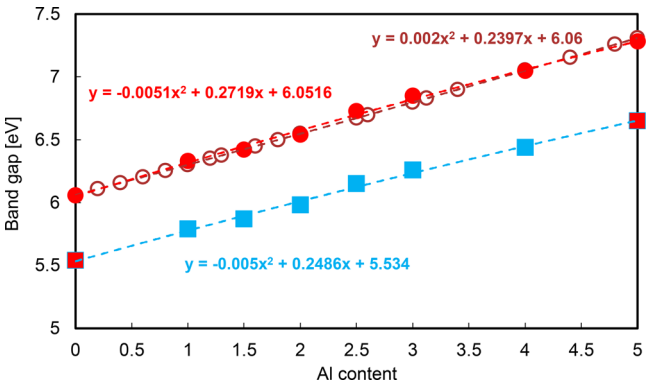

Figure 6. Fitting of experimental band gap data of $Y_3(Al_xGa_{(1-x)})_5O_{12}$) as a function of Al composition in the garnet by means of eqs 8a−8d. Experimental (azure square symbols) E^{fa} values (Tauc optical gap) and optical band gap values of YGG and YAG (red square at $mx_{Al} = 0$ and $mx_{Al} = 5$) are those derived from eqs 12a and 12b in the text. Experimental band gap values of YAGG samples as a function of composition derived from E^{fa} values (see text) have been reported in the figure (filled red circle). Theoretical band gap values (open circles) have been derived by using eqs 8a−8d, with E_{g1T} (7.28 eV) and E_{g2T} (6.04 eV) values derived in Figures 1 and 3, and $A_{2T,av} = 1.8775$; $B_{2Tav} = -1.84625$ eV; $\chi_{T2av} = 1.45$; $A_{1T,av} = 2.040625$; $B_{1Tav} = -1.824375$ eV; $\chi_{T2av} = 1.3875$.

values (azure squares) from the literature[55] for YAGG:Ce^{3+} crystals as a function of Al content in the interval of composition previously used in Figure 5 ($1 < mx_{Al} < 4$) together with the E^{fa} values of the YAGG end terms YGG (5.54 eV) and YAG (6.65 eV) (red squares) obtained from eqs 12a & 12b.

In the same figure (filled red circles) we report the E_g values, derived from experimental E^{fa} values (azure squares) by means of eqs 10a & 10d.

$$E_g = (E^{fa} + 0.25)^2 \times 0.008 + (E^{fa} + 0.25)\ [eV]$$

As for the experimental data, the following best-fitting quadratic equation was obtained

$$E_g = -0.005x^2 + 0.272x + 6.052[eV] R^2 = 0.996$$

with a bowing coefficient ($b = -0.005$) nearly to zero as evidenced by the almost linear behavior of line b.

The fitting (open brown circles) of the "experimental" E_g data reported in Figure 6 has been carried out by means of eqs 8 & 8a−8d by using as $E_{g,T2}$ for ternary $Y_3Ga_5O_{12}$ oxide, the room temperature E_g value (6.04 eV), previously calculated (see Figure 3). As for the other parameters entering eqs 8a−8d: χ_{2av}, A_{2Tav}, B_{2Tav} and χ_{1Tav}, $A_{1T,av}$, $B_{1T,av}$ (see figure captions), they have been calculated by using the weighted atomic averages of χ_i, A_i, B_i values used for fitting the $(Y_xAl_{(1-x)}O_3)$ and $(Y_xGa_{(1-x)}O_3)$ nonregular ternary oxide systems. The theoretical band gap values of YAGG in the entire range of composition ($0 \le mx_{Al} \le 5$) are in good agreement with experimental band gap values reported in the literature.[8−11,90] The best-fitting quadratic equation of theoretical data displays an R^2 coefficient equal to unity with a very low bowing parameter ($b = 0.002$). The very low value of the bowing parameter is not surprising if we take into consideration that

(a) as stressed in the case of regular and nonregular ternary oxides, the difference of the average electronegativity of the two end terms is the main factor in determining the value of the S_q and S_c terms (see eqs 6c & 6d and eqs 8c & 8d), which account for nonlinearity in the fitting equations.

(b) as for the end term YAG and YGG the difference of EN values $(\chi_{av(YAG)} - \chi_{av(YGG)}) = 0.0625$ is very small.

We have to say that, at variance with the results described above as well in older literature,[90] it has been suggested in a recent work[91] that there is a nonlinear behavior of the YAGG band gap as a function of the aluminum content in the garnet. A close inspection of the reported E_g values, calculated by using DFT-based techniques, reveals a strictly linear behavior of E_g (YAGG) versus x_{Al} for $mx_{Al} \le 4$, while for $mx_{Al} = 5$ a band gap value for $Y_3Al_5O_{12}$ lower than that estimated for $Y_3Al_4Ga_1O_{12}$ was obtained. In order to support such theoretical finding the authors report the values of E^{exc} versus mx_{al} at low

Table 2. Experimental E^{fa} and E^{exc} and Calculated E_g Values of $Lu_3(Ga_{1-x}Al_x)_5O_{12}$ from eqs 8 and 10a (see Figures 7−9)[a]

x_{Al}	$Lu_3(Ga_{1-x}Al_x)_5O_{12}$ (symbols and corresponding figures)	E_{exp}^{exc} (298 K)[89] azure open triangles (Figure 7)	$E_{g,calc}$ (298 K) from eq 10a filled azure triangles (Figure 8)	$E_{g,th}$ (298 K) from eq 8 open squares (Figure 8)	E_{exp}^{exc} (10 K)[8−11] open orange squares (Figure 7)	$E_{g,calc}$ (298 K) from eq 10b brown squares (Figure 9)	E_{exp}^{exc} (298 K)[92−96] green diamonds (Figure 9)	$E_{g,th}$ (298 K) from eq 8 open circles (Figure 9)	E_{exp}^{exc} (10 K)[92−96] green filled circles (Figure 7)
0	$Lu_3Ga_5O_{12}$	5.76	6.025	6.03	6.00	6.12	6.05	6.03	5.935
1	$Lu_3Ga_4AlO_{12}$	5.98	6.27	6.28	6.25	6.40	6.34	6.33	6.20
1.5	$Lu_3Ga_{3.5}Al_{1.5}O_{12}$								
2	$Lu_3Ga_2Al_2O_{12}$	6.28	6.60	6.55	6.50	6.67	6.62	6.62	6.46
2.5	$Lu_3Ga_{2.5}Al_{2.5}O_{12}$								
3	$Lu_3Ga_2Al_3O_{12}$	6.45	6.78	6.82	6.85	7.06	7.07	6.96	6.86
4	$Lu_3Ga_1Al_4O_{12}$	6.73	7.09	7.10	7.05	7.28	7.30	7.30	7.07
4.5	$Lu_3Ga_{0.5}Al_{4.5}O_{12}$						7.45	7.44	7.20
5	$Lu_3Al_5O_{12}$	6.99	7.38	7.40	7.35	7.61	7.54	7.60	7.28

[a]All the band gap values are expressed in electronvolts.

https://doi.org/10.1021/acs.jpcc.2c04523
J. Phys. Chem. C XXXX, XXX, XXX−XXX

temperature (T = 10 K) derived by Ueda et al. from the E_{fa} values of YAG:Ce^{3+} sample. In Figure S1 we report the difference of values $\Delta E_g = E_g(mx_{Al}) - E_g(x_{Al} = 0)$ from which a very good linearity and adaptation between experimental and theoretically estimated values of such difference is observed in all the range of composition. Although our results seem to exclude the observed decrease in the estimated E_g value for YAG, further investigations on the existence or not of such a dip in the plot of E_g versus mx_{Al}, at highest Al contents in YAGG, are welcome to clarify such a finding.

In Table 2 experimental and theoretical band gap values related to LuAGG compounds are summarized.

As for the LuAGG quaternary oxide system, we report in Figure 7 (blue open triangles) the experimental data set of

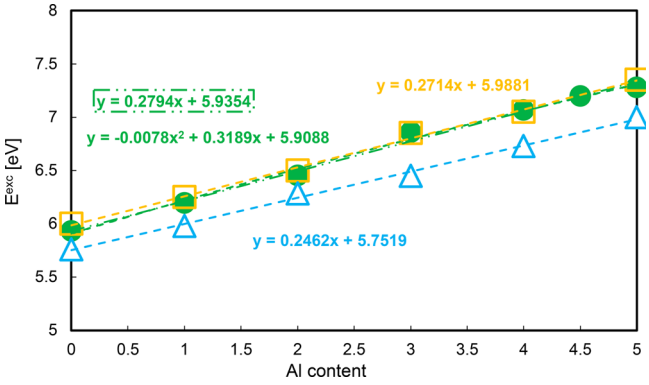

Figure 7. Experimental data sets of E^{exc} values for $Lu_3(Al_xGa_{(1-x)})_5O_{12}$ for $0 \le mx_{Al} \le 5$ derived from different sources (see text): azure open triangles data from ref 89 at RT, orange open square data from refs8−11 at 8−10 K, green filled circles data from refs 92−96 at 8−10 K.

optical band gap values of crystalline $Lu_3(Ga_{(1-x)}Al_x)_5O_{12}$ samples, doped with 1% Pr^{3+}, estimated at room temperature by Katelnikovas et al.[89] "by taking the value at half band intensity of the reflection spectra".

Before discussing the fitting procedure of the experimental data, we have to say that such a similar definition of band gap, but with reference to the excitation spectra, was also adopted in ref 92 where an optical band gap value of 7.214 eV, at 8 K, was reported for doped LuAG:0.1%Pr^{3+} crystal. It is interesting to note that, in ref 92, the study of the dependence of $E_{g,opt}$ from the temperature of LuAG:0.1%Pr^{3+} shows a difference of 0.143 eV in the $E_{g,opt}$ values on going from 8 to 300 K ($E_{g,opt}$ = 7.07 eV).[92] Previous studies by Zorenko et al.[93] evidenced that such ranges of photon energy pertain to the excitation peak energy, E^{exc}, of self-trapped excitons (STEs) generated in the host material rather than to the fundamental band gap of LuAG crystal. More recently E^{exc} values around 7.28−7.30 eV, at 8 K, have been attributed to the lowest-lying energy of STE in LuAG single crystals,[65,87] while an E^{exc} value of 7.15 eV, at 8 K, has been reported for the formation of STE in LuAG:Ce^{3+} doped crystal.[67] In summary, the experimental data[92−94] seem to suggest for LuAG a small decrease in the E^{exc} value from 7.28 to 7.20 eV with an increase in concentration of Pr^{3+} from zero to 0.1% and a further decrease of E^{exc} to 7.15 eV with a further increase of Pr^{3+} up to 1%. In the presence of Ce^{3+} ions E^{exc} values ranging from 7.25 to 7.15 eV have been reported for LuAG single crystals, while higher values up to 7.30 eV have been reported for LuAGG semiconducting films in absence of crystallographic defects usually present in a doped crystal.[94]

The value of 7.0 eV (see Figure 7 triangle at mx = 5) reported in ref 89 as "optical band gap" of LuAG:1% Pr, at room temperature, is in good agreement with the value of E_g reported by Ogieglo et al. (7.07 eV) for LuAG:0.1%Pr^{3+},[92] at room temperature, and it is coincident with the E^{exc} value of 7.15 eV, at 8 K, reported in ref 67 for LuAG:0.2 atom %Ce^{3+}, after correction for the difference of temperature according to eq 10a. According to this, and in agreement with other authors,[8−11] we will assume the values of E^{gopt} reported by Katelnikovas et al. as very good proxies of the room temperature E^{exc} values of LuAGG:1%Pr^{3+} crystalline samples.

For the sake of completeness, we plotted in Figure 7 also the E^{exc} values of LuAGG as a function of composition, obtained from measurements carried out at low temperature (8−10 K), reported by Dorenbos and co-workers (yellow squares) in several papers,[8−11] together with the experimental E^{exc} data set obtained by Fasoli et al.[95] for LuAGG samples, variously doped with Ce^{3+} and Eu^{3+}, at $mx_{Al} \ge 2$ (green circles). As for these last two data sets we have to say that, for mx_{Al} = 5, corresponding to pure LuAG, the value of 7.35 eV is reported by Dorenbos and co-workers[8−11] instead of the more recent one of 7.28 eV.[65] This last value has been used in the data set of Fasoli et al. owing to the difficulty of extracting this datum from the crowded inset of their Figure 2.[95] As for this set of data, moreover, the missing E^{exc} values, at mx_{Al} = 1 ($Lu_3Al_1Ga_4O_{12}$) and mx_{Al} = 0 ($Lu_3Ga_5O_{12}$), have been calculated by subtracting from the E^{exc} value of LuAGG the decrease in E_g values, ΔE_g, estimated by the authors from their PLE measurements reported in Figure 2 of ref 95. As for the E^{exc} value of $Lu_3Ga_5O_{12}$, estimated in such a way, it was in good agreement with the value calculated by means of eq 10c

$$E^{exc}(10\ K) = E^{fa}(RT) + 0.40\ eV = (5.53 + 0.40) \pm 0.05\ eV = 5.93 \pm 0.05\ eV$$

by using for LuGG the room-temperature E^{fa} value of 5.53 eV, corresponding to a value of light absorption coefficient $\alpha = 10^2$ cm^{-1} of LuGG single crystal in ref 96. All plotted data display a quite linear dependence of E^{exc} versus mx_{Al}, also in the region of highest Al content ($mx_{Al} \ge 4.5$), as evidenced by the linear best-fitting lines all displaying R^2 values (>0.99) nearly equal to 1 for the three data sets. A closer inspection of the original data of ref 95 shows a flattening in the E_g versus x_{Al} plot (see their Figure 2) owing to the lower band gap value assumed by the authors for LuAG with respect to the more recent value reported in the literature.[65]

In Figures 8 and 9 we report the electronic band gap values at room temperature, E_g(RT), obtained from the experimental data set of Figure 7, by using eq 10a in the case of values of E^{exc} measured at room temperature (Figure 8) or through eq 10b in the case of E^{exc} values measured at lowest temperatures (Figure 9).

The E_g data obtained from ref 89, although displaying a clear linear behavior, diverge appreciably in the E_g values from the two data sets derived from low-temperature E^{exc}. These last ones, apart from the small differences in the E_g values pertaining to the end terms LuAG and LuGG samples (see Figure 9), are practically coincident in the whole interval of composition ($1 \le mx_{Al} \le 4.5$).

In order to test the ability of our approach in fitting both these behaviors, and for the sake of brevity, we fitted in Figures 8 and 9 the two data sets (open triangles and open square

https://doi.org/10.1021/acs.jpcc.2c04523
J. Phys. Chem. C XXXX, XXX, XXX−XXX

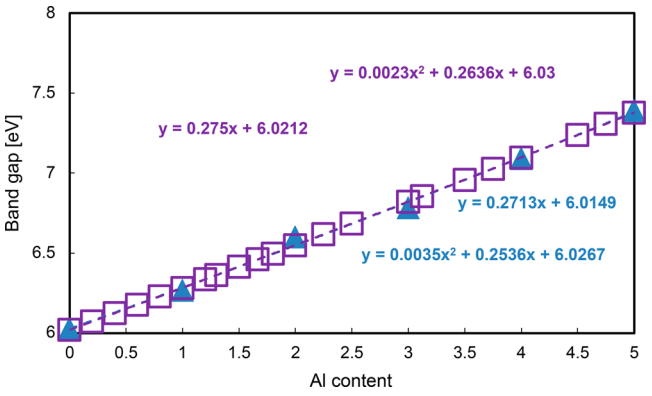

Figure 8. Fitting of experimental band gap data of LuAGG as a function of Al composition in the garnet by means of eqs 8a−8d (see text). In the figure experimental E_g values (azure triangle symbol), derived from E^{exc}(RT) values of Figure 7, have been reported together with the theoretical band gap values (open square symbol) derived by using eqs 8a−8d, with E_{g1T} (7.40 eV) and E_{g2T} (6.03 eV) values derived in Figure 4 and $A_{2T,av}$ = 1.8775; B_{2Tav} = −1.958 75 eV; χ_{T2av} = 1.438 75; $A_{1T,av}$ = 2.068 75; B_{1Tav} = −1.936 875 eV; χ_{T1av} = 1.376 25.

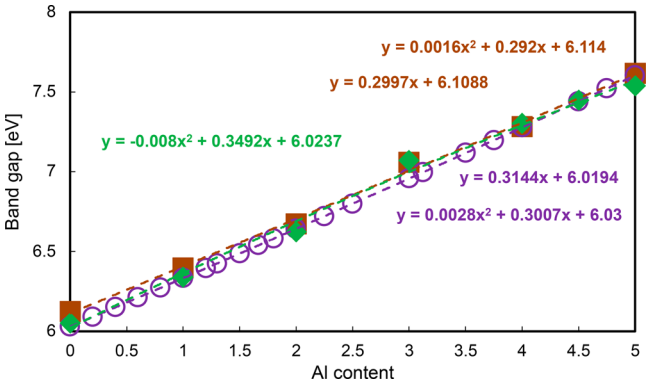

Figure 9. Fitting of experimental band gap values derived from E^{Exc} values obtained at 8 K reported in Figure 7. Fitting of experimental band gap data of LuAGG as a function of Al composition in the garnets by means of eqs 8a−8d (see text). In the figure experimental E_g(RT) values (brown square or green diamond symbol), derived from E^{exc}(8 K) values of Figure 7, have been reported together with the theoretical band gap values (open circles symbol) derived by using eqs 8 & 8a−8d, with E_{g1T} (7.60 eV) and E_{g2T} (6.03 eV) values derived in Figure 4 and $A_{2T,av}$ = 1.8775; B_{2Tav} = −1.95875 eV; χ_{T2av} = 1.43875; $A_{1T,av}$ = 2.1125; B_{1Tav} = −1.936875 eV; χ_{T1av} = 1.37625.

symbols in Figure 7) showing the largest divergence in E_g values of $Lu_3Al_5O_{12}$.

The E_g values of the two ternary end terms of Figures 8 and 9 are those calculated as in Figure 4 by fitting the two ternary systems $(Lu_{(1-x)}Al_x)_2O_3$ and $(Lu_{(1-x)}Ga_x)_2O_3$. The average A_{av}, B_{av}, χ_{av} values for the quaternary systems have been calculated according to eqs 7a−7c and reported in the caption of figures together with the band gap values of end terms E_{g2T} and E_{g1T}, LuGG and LuAG, respectively, of the LuAGG quaternary system. As for the fitting of E_g values reported in Figure 8, we used for k-alumina a value of E_g(RT) = 7.60 eV slightly larger than the value of 7.40 eV, calculated by Peitinger et al. and previously used in fitting the YAGG system but still in good agreement with the value of 7.67 eV reported for k-alumina by Seacat et al.[75]

A still larger E_g value (7.87 eV) of k-Al_2O_3 was employed to get a good agreement between the $E_{g,th}$ values, derived from eqs 8a−8d, and the experimental E_g(RT) values, derived from E^{exc}(8 K) values,[8,95] reported in Figure 9. This fact is evidenced by the larger value of the term $A_{1T,av}$ = (3 × 1.35 + 5 × 2.57)/8 = 2.1125 employed in fitting the E_g (RT) data (see caption) of Figure 9 with respect to Figure 8.

In absence of experimental data on the value of E_g for k-alumina the small difference in the band gap values between our theoretical values and experimental ones will be left unsolved, although the results of Figure 8 suggest a better agreement between our estimates, based on the existing values of k-alumina and the E^{exc} experimental data obtained at room temperature.

However, we like to stress that, from our fitting procedure of the experimental data of YAGG and LuAGG garnets, it is confirmed that k-alumina polymorph with a band gap E_g = (7.65 ± 0.25) eV is the suitable choice for a right estimation of the band gap values of $(Y,Lu)_3(Al_xGa_{1-x})_5O_{12}$ garnets.

5. CONCLUSIONS

A further generalization of our semiempirical approach to the modeling of the band gap of quaternary oxides has been carried out by showing the ability of this approach in providing very realistic values of band gap for mixed oxides on starting from the very simple initial correlation and by using the concept of average EN parameter for the metallic cations involved in the mixed oxides formation. This last concept previously used for ternary oxides has been shown to hold also for the investigated quaternary systems showing a difference of EN between the different cations entering in the oxides less than or equal to 0.45 unit in the Pauling scale. Further investigations involving different cations with a larger difference in the EN parameter could help to define the range of applicability of the proposed correlation to quaternary oxides. In previous work[4] on ternary oxide systems we reported that, in the presence of a large difference of EN ($\Delta\chi$ > 0.5−0.6 unit) between the two cations, the band gap of ternary oxide systems was, often, almost coincident with that of the binary oxides having a lower band gap. Further studies on quaternary oxides with cations spanning a larger range of EN values could be enlightening on such aspect.

Apart from any difference in the band gap values reported in the literature, owing to the use of different experimental techniques or theoretical approach, the presence of neglected or unevidenced excitonic effects seems to be a possible source of error in providing reliable agreement between experimental and theoretical E_g values. This has been evidenced in the fitting procedure of YGG and LuGG systems where a value of band gap for k-Ga_2O_3 equal to E_g = 5.42 ± 0.05 eV has been shown to be able in providing a good fitting of the quaternary (Y,Lu)AGG systems. It comes out that the actual optical band value (E_{gopt} = 4.95 ± 0.05 eV) reported for k-gallia should be assumed as an excitonic gap. Although this suggestion seems quite in agreement with the presence of excitons in β,α-Ga_2O_3 recently reported in the literature, further experimental investigations on the optical properties of k-gallia polymorph seem mandatory before accepting the suggestion derived from the fitting procedure of the ternary subsystems. Analogous considerations could be done as for the fundamental band gap value, E_g, of k-alumina, which, according to our approach, should display a band gap value comprised between 7.40 and 7.87 eV, with the recent reported value of 7.67 eV almost lying at the middle point. Owing to the intrinsic experimental uncertainty embodied in the E_g values data set of YAGG and

https://doi.org/10.1021/acs.jpcc.2c04523
J. Phys. Chem. C XXXX, XXX, XXX−XXX

LuAGG, the obtainment of a reliable experimental band gap value of k-alumina is a preliminary task for a possible physicochemical interpretation of the necessary variation of the $A_{1T,av}$ parameter for a best fitting of YAGG and LuAGG data. The eventual experimental confirmation of the band gap values of k-Al_2O_3 and k-Ga_2O_3 polymorphs, used to model the band gap dependence from the composition of the investigated garnets, could suggest the use of our approach to predict the band gap values of new polymorphs.

■ ASSOCIATED CONTENT

Supporting Information

The Supporting Information is available free of charge at https://pubs.acs.org/doi/10.1021/acs.jpcc.2c04523.

Unit formula volumes, *B* parameter and band gap values for Y_2O_3 polymorphs at room temperature; Unit formula volumes, *B* parameter and band gap values for Lu_2O_3 polymorphs at room temperature; Band gap variation of YAGG as a function of composition of the garnet (PDF)

■ AUTHOR INFORMATION

Corresponding Author

Francesco Di Quarto − *Dipartimento di Ingegneria, Viale delle Scienze, Università degli Studi di Palermo, 90128 Palermo, Italy;* orcid.org/0000-0001-8751-5928; Phone: +393204328592; Email: francesco.diquarto@unipa.it

Authors

Andrea Zaffora − *Dipartimento di Ingegneria, Viale delle Scienze, Università degli Studi di Palermo, 90128 Palermo, Italy;* orcid.org/0000-0002-4185-8308

Francesco Di Franco − *Dipartimento di Ingegneria, Viale delle Scienze, Università degli Studi di Palermo, 90128 Palermo, Italy;* orcid.org/0000-0002-5722-2881

Monica Santamaria − *Dipartimento di Ingegneria, Viale delle Scienze, Università degli Studi di Palermo, 90128 Palermo, Italy;* orcid.org/0000-0002-8690-4881

Complete contact information is available at: https://pubs.acs.org/10.1021/acs.jpcc.2c04523

Notes

The authors declare no competing financial interest.

■ ACKNOWLEDGMENTS

The authors thank Mrs. M. Rita Cinà for her support in providing many of the articles cited in References section and University of Palermo for the financial support.

■ REFERENCES

(1) Di Quarto, F.; Sunseri, C.; Piazza, S.; Romano, M. C. Semiempirical Correlation between Optical Band Gap Values of Oxides and the Difference of Electronegativity of the Elements. Its Importance for a Quantitative Use of Photocurrent Spectroscopy in Corrosion Studies. *J. Phys. Chem. B* **1997**, *101* (14), 2519−2525.

(2) Di Quarto, F.; Santamaria, M.; Sunseri, C.Photoelectrochemical Techniques in Corrosion Studies. In *Analytical Methods in Corrosion Science and Technology*;Marcus, P., Mansfeld, F., Eds.; Taylor & Francis Group: Boca Raton, FL, 2005; pp 697−732.

(3) Di Quarto, F.; La Mantia, F.; Santamaria, M.Physicochemical Characterization of Passive Films and Corrosion Layers by Differential Admittance and Photocurrent Spectroscopy. In *Modern Aspects of Electrochemistry, No. 46: Progress in Corrosion Science and Engineering I*;Pyun, S.-I., Lee, J.-W., Eds.; Springer: New York, 2009; pp 231−316.

(4) Quarto, F. D.; Zaffora, A.; Franco, F. D.; Santamaria, M. Critical Review - Photocurrent Spectroscopy in Corrosion and Passivity Studies: A Critical Assessment of the Use of Band Gap Value to Estimate the Oxide Film Composition. *J. Electrochem. Soc.* **2017**, *164* (12), C671−C681.

(5) Di Quarto, F.; Zaffora, A.; Di Franco, F.; Santamaria, M. A Generalized Semiempirical Approach to the Modeling of the Optical Band Gap of Ternary Al-(Ga, Nb, Ta, W) Oxides Containing Different Alumina Polymorphs. *Inorg. Chem.* **2021**, *60* (3), 1419−1435.

(6) Zaanen, J.; Sawatzky, G. A.; Allen, J. W. Band Gaps and Electronic Structure of Transition-Metal Compounds. *Phys. Rev. Lett.* **1985**, *55* (4), 418−421.

(7) Zaanen, J.; Sawatzky, G. A. Systematics in Band Gaps and Optical Spectra of 3D Transition Metal Compounds. *J. Solid State Chem.* **1990**, *88* (1), 8−27.

(8) Dorenbos, P. Electronic Structure and Optical Properties of the Lanthanide Activated RE3$(Al_{1-x}Ga_x)_5O_{12}$ (RE = Gd, Y, Lu) Garnet Compounds. *J. Lumin.* **2013**, *134*, 310−318.

(9) Awater, R. H. P.; Dorenbos, P. The Bi^{3+} 6s and 6p Electron Binding Energies in Relation to the Chemical Environment of Inorganic Compounds. *J. Lumin.* **2017**, *184*, 221−231.

(10) Dorenbos, P. Charge Transfer Bands in Optical Materials and Related Defect Level Location. *Opt. Mater. (Amst).* **2017**, *69*, 8−22.

(11) Ueda, J.; Tanabe, S. Review of Luminescent Properties of Ce^{3+}-Doped Garnet Phosphors: New Insight into the Effect of Crystal and Electronic Structure. *Opt. Mater. X* **2019**, *1*, 100018.

(12) Krasnikov, A.; Mihokova, E.; Nikl, M.; Zazubovich, S.; Zhydachevskyy, Y. Luminescence Spectroscopy and Origin of Luminescence Centers in Bi-Doped Materials. *Crystals* **2020**, *10* (3), 208.

(13) Singh, C. N.; Pilania, G.; Bárta, J.; Uberuaga, B. P.; Liu, X. Y. Accurately Predicting Optical Properties of Rare-Earth, Aluminate Scintillators: Influence of Electron−Hole Correlation. *J. Mater. Chem. C* **2021**, *9* (23), 7292−7301.

(14) Pauling, L.*The Nature of Chemical Bond*;Cornell University Press: Ithaca, NY, 1959.

(15) Allred, A. L. Electronegativity Values from Thermochemical Data. *J. Inorg. Nucl. Chem.* **1961**, *17* (3−4), 215−221.

(16) Little, E. J.; Jones, M. M. A Complete Table of Electronegativities. *J. Chem. Educ.* **1960**, *37* (5), 231−233.

(17) Mann, J. B.; Meek, T. L.; Knight, E. T.; Capitani, J. F.; Allen, L. C. Configuration Energies of the d-Block Elements. *J. Am. Chem. Soc.* **2000**, *122* (21), 5132−5137.

(18) Rahm, M.; Zeng, T.; Hoffmann, R. Electronegativity Seen as the Ground-State Average Valence Electron Binding Energy. *J. Am. Chem. Soc.* **2019**, *141* (1), 342−351.

(19) Morss, L. R. Thermochemical Properties of Yttrium, Lanthanum, and the Lanthanide Elements and Ions. *Chem. Rev.* **1976**, *76* (6), 827−841.

(20) Zinkevich, M. Thermodynamics of Rare Earth Sesquioxides. *Prog. Mater. Sci.* **2007**, *52* (4), 597−647.

(21) Wu, B.; Zinkevich, M.; Aldinger, F.; Wen, D.; Chen, L. Ab Initio Study on Structure and Phase Transition of A- and B-Type Rare-Earth Sesquioxides Ln_2O_3 (Ln = La−Lu, Y, and Sc) Based on Density Function Theory. *J. Solid State Chem.* **2007**, *180* (11), 3280−3287.

(22) Richard, D.; Errico, L. A.; Rentería, M. Structural Properties and the Pressure-Induced C → A Phase Transition of Lanthanide Sesquioxides from DFT and DFT + U Calculations. *J. Alloys Compd.* **2016**, *664*, 580−589.

(23) Kimura, S.-i.; Arai, F.; Ikezawa, M. Optical Study on Electronic Structure of Rare-Earth Sesquioxides. *J. Phys. Soc. Jpn.* **2000**, *69* (10), 3451−3457.

(24) Yusa, H.; Tsuchiya, T.; Sata, N.; Ohishi, Y. Dense Yttria Phase Eclipsing the A-Type Sesquioxide Structure: High-Pressure Experi-

ments and Ab Initio Calculations. *Inorg. Chem.* **2010**, *49* (10), 4478−4485.
(25) Jiang, S.; Liu, J.; Li, X.-D.; Li, Y.-C.; He, S.-M.; Zhang, J.-C.; et al. High-Pressure Phase Transitions of Cubic Y_2O_3 under High Pressures by In-Situ Synchrotron X-Ray Diffraction. *Chin. Phys. Lett.* **2019**, *36* (4), 46103.
(26) Glasser, L. Solid-State Energetics and Electrostatics: Madelung Constants and Madelung Energies. *Inorg. Chem.* **2012**, *51* (4), 2420−2424.
(27) Emeline, A. V.; Kataeva, G. V.; Ryabchuk, V. K.; Serpone, N. Photostimulated Generation of Defects and Surface Reactions on a Series of Wide Band Gap Metal-Oxide Solids. *J. Phys. Chem. B* **1999**, *103* (43), 9190−9199.
(28) Mudavakkat, V. H.; Atuchin, V. V.; Kruchinin, V. N.; Kayani, A.; Ramana, C. V. Structure, Morphology and Optical Properties of Nanocrystalline Yttrium Oxide (Y_2O_3) Thin Films. *Opt. Mater. (Amst)* **2012**, *34* (5), 893−900.
(29) Razavi-Khosroshahi, H.; Edalati, K.; Emami, H.; Akiba, E.; Horita, Z.; Fuji, M. Optical Properties of Nanocrystalline Monoclinic Y_2O_3 Stabilized by Grain Size and Plastic Strain Effects via High-Pressure Torsion. *Inorg. Chem.* **2017**, *56* (5), 2576−2580.
(30) Badehian, H. A.; Salehi, H.; Ghoohestani, M. First-Principles Study of Elastic, Structural, Electronic, Thermodynamical, and Optical Properties of Yttria (Y_2O_3) Ceramic in Cubic Phase. *J. Am. Ceram. Soc.* **2013**, *96* (6), 1832−1840.
(31) Sarmadian, N.; Saniz, R.; Partoens, B.; Lamoen, D.; Volety, K.; Huyberechts, G.; Paul, J. High Throughput First-Principles Calculations of Bixbyite Oxides for TCO Applications. *Phys. Chem. Chem. Phys.* **2014**, *16* (33), 17724−17733.
(32) Ahuja, B. L.; Sharma, S.; Heda, N. L.; Tiwari, S.; Kumar, K.; Meena, B. S.; Bhatt, S. Electronic and Optical Properties of Ceramic Sc_2O_3 and Y_2O_3: Compton Spectroscopy and First Principles Calculations. *J. Phys. Chem. Solids* **2016**, *92*, 53−63.
(33) Zhang, X.; Gao, S.; Gui, W.; Zeng, Q. First-Principles Study of Structure, Mechanical and Optical Properties of La- and Sc-Doped Y_2O_3. *J. Rare Earths* **2019**, *37* (8), 879−885.
(34) Hinuma, Y.; Gake, T.; Oba, F. Band Alignment at Surfaces and Heterointerfaces of Al_2O_3, Ga_2O_3, In_2O_3, and Related Group-III Oxide Polymorphs: A First-Principles Study. *Phys. Rev. Mater.* **2019**, *3* (8), 084605.
(35) Chen, S.; Xie, Y.; Feng, H.; Guo, H. Band Structures of RE_2O_3:Eu (RE = Lu, Y, Sc) from Perspective of Spin-Polarized Quasi-Particle Approximation. *Model. Simul. Mater. Sci. Eng.* **2021**, *29* (6), 065002.
(36) Guzik, M.; Pejchal, J.; Yoshikawa, A.; Ito, A.; Goto, T.; Siczek, M.; Lis, T.; Boulon, G. Structural Investigations of Lu_2O_3 as Single Crystal and Polycrystalline Transparent Ceramic. *Cryst. Growth Des.* **2014**, *14* (7), 3327−3334.
(37) *CRC Handbook of Chemistry and Physics,*90th ed.; Lide, D. R., Ed.; CRC Press/Taylor and Francis: Boca Raton, FL, 2010.
(38) den Engelsen, D.; Ireland, T. G.; Dhillon, R.; Fern, G.; Harris, P. G.; Silver, J. Red Shift of CT-Band in Cubic Y_2O_3:Eu^{3+} upon Increasing the Eu^{3+} Concentration. *ECS J. Solid State Sci. Technol.* **2016**, *5* (5), R59.
(39) Prokofiev, A. V.; Shelykh, A. I.; Melekh, B. T. Periodicity in the Band Gap Variation of Ln_2X_3 (X = O, S, Se) in the Lanthanide Series. *J. Alloys Compd.* **1996**, *242* (1−2), 41−44.
(40) Xiong, K.; Robertson, J. Electronic Structure of Oxygen Vacancies in La_2O_3, Lu_2O_3 and $LaLuO_3$. *Microelectron. Eng.* **2009**, *86* (7−9), 1672−1675.
(41) Huang, B. 4f Fine-Structure Levels as the Dominant Error in the Electronic Structures of Binary Lanthanide Oxides. *J. Comput. Chem.* **2016**, *37* (9), 825−835.
(42) Jiang, H.; Rinke, P.; Scheffler, M. Electronic Properties of Lanthanide Oxides from the GW Perspective. *Phys. Rev. B - Condens. Matter Mater. Phys.* **2012**, *86* (12), 125115.
(43) Gillen, R.; Clark, S. J.; Robertson, J. Nature of the Electronic Band Gap in Lanthanide Oxides. *Phys. Rev. B - Condens. Matter Mater. Phys.* **2013**, *87* (12), 125116.
(44) Seguini, G.; Bonera, E.; Spiga, S.; Scarel, G.; Fanciulli, M. Energy-Band Diagram of Metal/Lu_2O_3/Silicon Structures. *Appl. Phys. Lett.* **2004**, *85* (22), 5316.
(45) Moore, C. A.; Brown, D. C.; Sanjeewa, L. D.; McMillen, C. D.; Kolis, J. W. Yb:Lu_2O_3 Hydrothermally-Grown Single-Crystal and Ceramic Absorption Spectra Obtained between 298 and 80 K. *J. Lumin.* **2016**, *174*, 29−35.
(46) Hattori, T.; Yoshida, T.; Shiraishi, T.; Takahashi, K.; Nohira, H.; Joumori, S.; Nakajima, K.; Suzuki, M.; Kimura, K.; Kashiwagi, I.; et al. Composition, Chemical Structure, and Electronic Band Structure of Rare Earth Oxide/Si(1 0 0) Interfacial Transition Layer. *Microelectron. Eng.* **2004**, *72* (1−4), 283−287.
(47) Nohira, H.; Shiraishi, T.; Nakamura, T.; Takahashi, K.; Takeda, M.; Ohmi, S.; Iwai, H.; Hattori, T. Chemical and Electronic Structures of Lu_2O_3/Si Interfacial Transition Layer. *Appl. Surf. Sci.* **2003**, *216* (1−4), 234−238.
(48) Kaichev, V. V.; Asanova, T. I.; Erenburg, S. B.; Perevalov, T. V.; Shvets, V. A.; Gritsenko, V. A. Atomic and Electronic Structures of Lutetium Oxide Lu_2O_3. *J. Exp. Theor. Phys. 2013 1162* **2013**, *116* (2), 323−329.
(49) Wang, Z.; Zhang, W.; Lin, L.; You, B.; Fu, Y.; Yin, M. Preparation and Spectroscopic Characterization of Lu_2O_3:Eu^{3+} Nanopowders and Ceramics. *Opt. Mater. (Amst)* **2008**, *30* (10), 1484−1488.
(50) Zych, E.; Trojan-Piegza, J. Low-Temperature Luminescence of Lu_2O_3:Eu Ceramics upon Excitation with Synchrotron Radiation in the Vicinity of Band Gap Energy. *Chem. Mater.* **2006**, *18* (8), 2194−2199.
(51) Zych, E.; Wójtowicz, M.; Kępiński, L.; Małecka, M. A. Size Effects in the Low Temperature Spectroscopy of Lu_2O_3 Nanopowders. *Opt. Mater. (Amst)* **2008**, *31* (2), 241−246.
(52) Dorenbos, P. The Electronic Level Structure of Lanthanide Impurities in REPO4, REBO3, REAlO3, and RE2O3 (RE = La, Gd, Y, Lu, Sc) Compounds. *J. Phys.: Condens. Matter* **2013**, *25* (22), 225501.
(53) Tomiki, T.; Tamashiro, J.; Tanahara, Y.; Yamada, A.; Fukutani, H.; Miyahara, T.; Kato, H.; Shin, S.; Ishigame, M. Optical Spectra of Y_2O_3 Single Crystals in VUV. *J. Phys. Soc. Jpn.* **1986**, *55* (12), 4543−4549.
(54) Tomiki, T.; Shikenbaru, T.; Ganaha, Y.; Futemma, T.; Kato, H.; Yuri, M.; Yuri, M.; Fukutani, H.; Miyahara, T.; Shin, S.; et al. Optical Spectra of Y_2O_3 Single Crystals in the Vacuum Ultraviolet Region. II. *J. Phys. Soc. Jpn.* **1992**, *61* (8), 2951−2963.
(55) Ueda, J.; Dorenbos, P.; Bos, A. J. J.; Kuroishi, K.; Tanabe, S. Control of Electron Transfer between Ce^{3+} and Cr^{3+} in the $Y_3Al_{5-x}Ga_xO_{12}$ Host via Conduction Band Engineering. *J. Mater. Chem. C* **2015**, *3* (22), 5642−5651.
(56) Ueda, J.; Meijerink, A.; Dorenbos, P.; Bos, A. J. J.; Tanabe, S. Thermal Ionization and Thermally Activated Crossover Quenching Processes for 5d-4f Luminescence in $Y_3Al_{5-x}Ga_xO_{12}$:Pr^{3+}. *Phys. Rev. B* **2017**, *95* (1), 014303.
(57) Kittel, C.*Introduction to Solid State Physics,*8th ed.; John Wiley & Sons Inc., 2004.
(58) Mott, N. F.; Davis, E. A.*Electronic Processes in Non-Crystalline Materials;*Clarendon Press: Oxford, U.K., 1971.
(59) Slack, G. A.; Oliver, D. W.; Chrenko, R. M.; Roberts, S. Optical Absorption of $Y_3Al_5O_{12}$ from 10- to 55000 cm^{-1} Wave Numbers. *Phys. Rev.* **1969**, *177* (3), 1308.
(60) Robbins, D. J.; Cockayne, B.; Lent, B.; Glasper, J. L. Comparison of Theoretical and Measured Efficiencies for Tb^{3+} -Activated Garnet Oxide Phosphors. *Solid State Commun.* **1980**, *36* (8), 691−693.
(61) Tomiki, T.; Isa, Y.; Kadekawa, Y.; Ganaha, Y.; Toyokawa, N.; Miyazato, T.; Miyazato, M.; Kohatsu, T.; Shimabukuro, H.; Tamashiro, J. Optical Absorption of Single Crystals of $Y_3Al_5O_{12}$ and $Y_3Al_5O_{12}$:Nd^{3+} in the UV Fundamental Absorption Edge Region. *J. Phys. Soc. Jpn.* **1996**, *65* (4), 1106−1113.
(62) Ueda, J.; Tanabe, S.; Nakanishi, T. Analysis of Ce^{3+} Luminescence Quenching in Solid Solutions between $Y_3Al_5O_{12}$ and

https://doi.org/10.1021/acs.jpcc.2c04523
J. Phys. Chem. C XXXX, XXX, XXX−XXX

$Y_3Ga_5O_{12}$ by Temperature Dependence of Photoconductivity Measurement. *J. Appl. Phys.* **2011**, *110* (5), 053102.
(63) Zorenko, Y.; Zorenko, T.; Vistovskyy, V.; Grinberg, M.; Łukasiewicz, T. Time-Resolved Spectroscopy of Intrinsic Luminescence of $Y_3Ga_5O_{12}$ and $(LaLu)_3Lu_2Ga_3O_{12}$ Single Crystals. *Opt. Mater. (Amst)* **2009**, *31* (12), 1835−1838.
(64) Zorenko, Y. V.; Voloshinovskii, A. S.; Stryganyuk, G. M.; Konstankevych, I. V. Ultraviolet Luminescence of Single Crystals and Single-Crystal Films of YAlO3. *Opt. Spectrosc.* **2004**, *96* (1), 70−76.
(65) Bartosiewicz, K.; Horiai, T.; Yamaji, A.; Yoshikawa, A.; Kurosawa, S.; Kim, K. J.; Vistovskyy, V.; Voloshinovskii, A.; Zorenko, Y. Bright Exciton Luminescence from La Doped $Lu_3Al_5O_{12}$ Single Crystals. *J. Lumin.* **2021**, *235*, 118013.
(66) Ning, L.; Tanner, P. A.; Harutunyan, V. V.; Aleksanyan, E.; Makhov, V. N.; Kirm, M. Luminescence and Excitation Spectra of YAG:Nd^{3+} Excited by Synchrotron Radiation. *J. Lumin.* **2007**, *127* (2), 397−403.
(67) Zorenko, T.; Gorbenko, V.; Witkiewicz-Lukaszek, S.; Zorenko, Y. Luminescent Properties of $(La,Lu,Gd)_3(Al,Sc,Ga)_5O_{12}$:Ce Mixed Garnets under Synchrotron Radiation Excitation. *J. Lumin.* **2018**, *199*, 483−487.
(68) Kirm, M.; Lushchik, A.; Lushchik, C.; Zimmerer, G. Investigation of Luminescence Properties of Pure and Ce^{3+} Doped $Y_3Al_5O_{12}$ Crystals Using VUV Radiation. *ECS Proc.* **2000**, *99* (40), 113−122.
(69) Abramov, V. N.; Kuznetsov, A. I. Fundamental Absorption of Y_2O_3 and $YAlO_3$. *Sov Phys. Solid State* **1978**, *20* (3), 399−402.
(70) Kwok, C.; Aita, C. R.; Kolawa, E. Process Parameter-growth Environment-film Property Relationships for the Sputter Deposited Yttrium−Oxygen System. *J. Vac. Sci. Technol. A Vacuum, Surfaces, Film.* **1990**, *8* (3), 1330.
(71) Kaminaga, K.; Oka, D.; Hasegawa, T.; Fukumura, T. New Lutetium Oxide: Electrically Conducting Rock-Salt LuO Epitaxial Thin Film. *ACS Omega* **2018**, *3* (10), 12501−12504.
(72) Zhan, X.; Li, Z.; Liu, B.; Wang, J.; Zhou, Y.; Hu, Z. Theoretical Prediction of Elastic Stiffness and Minimum Lattice Thermal Conductivity of $Y_3Al_5O_{12}$, $YAlO_3$ and $Y_4Al_2O_9$. *J. Am. Ceram. Soc.* **2012**, *95* (4), 1429−1434.
(73) Xia, Z.; Meijerink, A. Ce^{3+}-Doped Garnet Phosphors: Composition Modification, Luminescence Properties and Applications. *Chem. Soc. Rev.* **2017**, *46* (1), 275−299.
(74) Peintinger, M. F.; Kratz, M. J.; Bredow, T. Quantum-Chemical Study of Stable, Meta-Stable and High-Pressure Alumina Polymorphs and Aluminum Hydroxides. *J. Mater. Chem. A* **2014**, *2* (32), 13143−13158.
(75) Seacat, S.; Lyons, J. L.; Peelaers, H. Properties of Orthorhombic Ga_2O_3 Alloyed with In_2O_3 and Al2O3. *Appl. Phys. Lett.* **2021**, *119* (4), 042104.
(76) Chandran, C. V.; Kirschhock, C. E. A.; Radhakrishnan, S.; Taulelle, F.; Martens, J. A.; Breynaert, E. Alumina: Discriminative Analysis Using 3D Correlation of Solid-State NMR Parameters. *Chem. Soc. Rev.* **2019**, *48* (1), 134−156.
(77) Ayoola, H. O.; House, S. D.; Bonifacio, C. S.; Kisslinger, K.; Saidi, W. A.; Yang, J. C. Evaluating the Accuracy of Common γ-Al_2O_3 Structure Models by Selected Area Electron Diffraction from High-Quality Crystalline γ-Al2O3. *Acta Mater.* **2020**, *182*, 257−266.
(78) Sun, H.; Li, K. H.; Castanedo, C. G. T.; Okur, S.; Tompa, G. S.; Salagaj, T.; Lopatin, S.; Genovese, A.; Li, X. HCl Flow-Induced Phase Change of α-, β-, and ϵ-Ga_2O_3 Films Grown by MOCVD. *Cryst. Growth Des.* **2018**, *18* (4), 2370−2376.
(79) Oshima, Y.; Víllora, E. G.; Matsushita, Y.; Yamamoto, S.; Shimamura, K. Epitaxial Growth of Phase-Pure ϵ-Ga_2O_3 by Halide Vapor Phase Epitaxy. *J. Appl. Phys.* **2015**, *118* (8), 085301.
(80) Kneiß, M.; Hassa, A.; Splith, D.; Sturm, C.; Von Wenckstern, H.; Schultz, T.; Koch, N.; Lorenz, M.; Grundmann, M. Tin-Assisted Heteroepitaxial PLD-Growth of κ-Ga_2O_3 Thin Films with High Crystalline Quality. *APL Mater.* **2019**, *7* (2), 022516.
(81) Furthmüller, J.; Bechstedt, F. Quasiparticle Bands and Spectra of Ga_2O_3 Polymorphs. *Phys. Rev. B* **2016**, *93*, 115204.
(82) Kaneko, K.; Fujita, S. Novel P-Type Oxides with Corundum Structure for Gallium Oxide Electronics. *J. Mater. Res.* **2022**, *37* (3), 651−659.
(83) Segura, A.; Artús, L.; Cuscó, R.; Goldhahn, R.; Feneberg, M. Band Gap of Corundumlike α-Ga_2O_3 Determined by Absorption and Ellipsometry. *Phys. Rev. Mater.* **2017**, *1*, 024604.
(84) Yamaoka, S.; Nakayama, M. Evidence for Formation of Self-Trapped Excitons in a β-Ga_2O_3 Single Crystal. *Phys. status solidi* **2016**, *13* (2−3), 93−96.
(85) Pues, P.; Laube, M.; Fischer, S.; Schröder, F.; Schwung, S.; Rytz, D.; Fiehler, T.; Wittrock, U.; Jüstel, T. Luminescence and Up-Conversion of Single Crystalline $Lu_3Al_5O_{12}:Pr^{3+}$. *J. Lumin.* **2021**, *234*, 117987.
(86) Nikl, M.; Yoshikawa, A.; Kamada, K.; Nejezchleb, K.; Stanek, C. R.; Mares, J. A.; Blazek, K. Development of LuAG-Based Scintillator Crystals − A Review. *Prog. Cryst. Growth Charact. Mater.* **2013**, *59* (2), 47−72.
(87) Hu, C.; Feng, X.; Li, J.; Ge, L.; Zhang, Y.; Kou, H.; Xu, J.; Pan, Y. Fabrication, Optical and Scintillation Properties of $(Lu_{0.75},Y_{0.25})$-AG:Pr Ceramic Scintillators. *Opt. Mater. (Amst)* **2017**, *69*, 214−218.
(88) Babin, V.; Krasnikov, A.; Maksimov, Y.; Nejezchleb, K.; Nikl, M.; Savikhina, T.; Zazubovich, S. Luminescence of Pr^{3+}-Doped Garnet Single Crystals. *Opt. Mater. (Amst)* **2007**, *30* (1), 30−32.
(89) Katelnikovas, A.; Bettentrup, H.; Dutczak, D.; Kareiva, A.; Jüstel, T. On the Correlation between the Composition of Pr^{3+} Doped Garnet Type Materials and Their Photoluminescence Properties. *J. Lumin.* **2011**, *131* (12), 2754−2761.
(90) Mayolet, A.; Zhang, W.; Simoni, E.; Krupa, J. C.; Martin, P. Investigation in the VUV Range of the Excitation Efficiency of the Tb^{3+} Ion Luminescence in Y_3 $(Al_x$, $Ga_y)5O_{12}$ Host Lattices. *Opt. Mater. (Amst)* **1995**, *4* (6), 757−769.
(91) Vrubel, I. I.; Polozkov, R. G.; Shelykh, I. A.; Khanin, V. M.; Rodnyi, P. A.; Ronda, C. R. Bandgap Engineering in Yttrium-Aluminum Garnet with Ga Doping. *Cryst. Growth Des.* **2017**, *17* (4), 1863−1869.
(92) Ogiegło, J. M.; Zych, A.; Jüstel, T.; Meijerink, A.; Ronda, C. R. Luminescence and Energy Transfer in $Lu_3Al_5O_{12}$ Scintillators Co-Doped with Ce^{3+} and Pr^{3+}. *Opt. Mater. (Amst)* **2013**, *35* (3), 322−331.
(93) Zorenko, Y.; Voznyak, T.; Gorbenko, V.; Zorenko, T.; Voloshinovskii, A.; Vistovsky, V.; Nikl, M.; Nejezchleb, K.; Kolobanov, V.; Spasskii, D. Luminescence Spectroscopy of Excitons and Antisite Defects in $Lu_3Al_5O_{12}$ Single Crystals and Single-Crystal Films. *Opt. Spectrosc.* **2008**, *104* (1), 75−87.
(94) Babin, V.; Bichevin, V.; Gorbenko, V.; Kink, M.; Makhov, A.; Maksimov, Y.; Nikl, M.; Stryganyuk, G.; Zazubovich, S.; Zorenko, Y. Time-Resolved Spectroscopy of Exciton-Related States in Single Crystals and Single Crystalline Films of $Lu_3Al_5O_{12}$ and $Lu_3Al_5O_{12}$:Ce. *Phys. status solidi* **2011**, *248* (6), 1505−1512.
(95) Fasoli, M.; Vedda, A.; Nikl, M.; Jiang, C.; Uberuaga, B. P.; Andersson, D. A.; McClellan, K. J.; Stanek, C. R. Band-Gap Engineering for Removing Shallow Traps in Rare-Earth $Lu_3Al_5O_{12}$ Garnet Scintillators Using Ga_3 + Doping. *Phys. Rev. B - Condens. Matter Mater. Phys.* **2011**, *84* (8), 081102.
(96) Mihokova, E.; Vedda, A.; Fasoli, M.; Moretti, F.; Bulin, A. L.; Nikl, M.; Bettinelli, M.; Speghini, A.; Ogino, H.; Yoshikawa, A. Defect States in $Lu_3Ga_xAl_{5-x}O_{12}$ Crystals and Powders. *Opt. Mater. (Amst)* **2010**, *32* (10), 1298−1301.
(97) van Pieterson, L.; Heeroma, M.; de Heer, E.; Meijerink, A. Charge transfer luminescence of Yb^{3+}. *J. Lumin.* **2000**, *91* (3−4), 177−183.
(98) Laube, M.; den Engelsen, D.; Jansen, T.; Fern, G.; Harris, P.; Ireland, T.; Silver, J.; Jüstel, T. On the Photo- and Cathodoluminescence of LaB_3O_6:Gd,Bi, $Y_3Al_5O_{12}$:Pr, $Y_3Al_5O_{12}$:Gd, $Lu_3Al_5O_{12}$:Pr, and $Lu_3Al_5O_{12}$:Gd. *ECS J. Solid State Sci. Technol.* **2018**, *7* (12), R206.
(99) Zorenko, T.; Gorbenko, V.; Nizankovskiy, S.; Zorenko, Yu. Comparison of the luminescent properties of $Y_3Al_5O_{12}$:Pr crystals and films. *Acta Phys. Polym.* **2018**, *133* (4), 948−953.

https://doi.org/10.1021/acs.jpcc.2c04523
J. Phys. Chem. C XXXX, XXX, XXX−XXX

(100) Zorenko, Yu; Voloshinovskii, A.; Savchyn, V.; Voznyak, T.; Nikl, M.; Nejezchleb, K.; Mikhailin, V.; Kolobanov, V.; Spassky, D. Exciton and antisite defect-related luminescence in $Lu_3Al_5O_{12}$ and $Y_3Al_5O_{12}$ garnets. *Phys. status solidi* **2007**, *244* (6), 2180−2189.

https://doi.org/10.1021/acs.jpcc.2c04523
J. Phys. Chem. C XXXX, XXX, XXX−XXX